

Chapter 2

Electron Emission from Dust

2.1 Free Electron Model

2.1.1 Basic Model

The free electron model, which is applicable to metals, is based on the fact that the valence electrons in a metal get detached from atoms and are free to move around in the metal and that their motion is not affected by the ions and other electrons. The confinement of the free electrons in the metal is ensured by a potential energy barrier of height W_a at the surface, corresponding to energy, much larger than the mean energy of the free electrons in the metal. The potential energy of the electrons within the metal is assumed to be uniform; it is often, without loss of generality taken as zero or $-W_a$.

2.1.2 Density of Electronic States

Wave mechanics provides an effective basis for the understanding of processes on the atomic scale. The wave mechanical approach is necessary to appreciate a host of phenomena, related to the behavior of electrons in a solid.

It is well known that electrons with a momentum \mathbf{p} display wave phenomena with an associated wave vector \mathbf{k} , given by

$$\mathbf{k} = (2\pi/h)\mathbf{p}, \quad (2.1)$$

where h is *Planck's* constant.

One may associate a parameter ψ with the wave motion so that the probability of occurrence of an electron in the volume element $dx dy dz$ is $\psi\psi^* dx dy dz$; the function ψ satisfies *Schrödinger's* equation

$$\nabla^2\psi + (8\pi^2 m_e/h^2)[E - V(x, y, z)]\psi = 0, \quad (2.2)$$

where E and V denote the total and potential energy of the electron and m_e is the mass of the electron.

Schrödinger's equation has stood the test of time and led to a host of experimentally verified results.

In a metallic crystal (with dimensions of many atomic spacings) having a periodicity L_x , L_y , and L_z in the x , y , and z directions, ψ has a periodic solution of the form (for $V = 0$)

$$\psi(x, y, z) = A \exp[i(k_x x + k_y y + k_z z)], \quad (2.3a)$$

such that

$$\psi[(x + L_x), (y + L_y), (z + L_z)] = \psi(x, y, z). \quad (2.3b)$$

Equations (2.3a) and (2.3b) lead to $k_x L_x = 2n_x \pi$, $k_y L_y = 2n_y \pi$ and $k_z L_z = 2n_z \pi$. Substituting for k , from (2.1) in the above relations one gets

$$p_x = n_x h / L_x, \quad p_y = n_y h / L_y \quad \text{and} \quad p_z = n_z h / L_z, \quad (2.4)$$

where n_x , n_y , and n_z are integers.

In the volume element $L_x L_y L_z$ an electronic state is characterized by a set of integral values of n_x , n_y , and n_z . In this volume consider an element $\Delta n_x \Delta n_y \Delta n_z$ such that n_x lies between n_x and $n_x + \Delta n_x$, n_y lies between n_y and $n_y + \Delta n_y$ and n_z lies between n_z and $n_z + \Delta n_z$; within this element n_x can have Δn_x values, n_y can have Δn_y values and n_z can have Δn_z values. Hence by *Pauli's* exclusion principle (which stipulates a unique set of four quantum numbers for an electron) the number of electronic states (characterized by a definite combination of n_x , n_y , n_z and the spin quantum number) in this element is $2\Delta n_x \Delta n_y \Delta n_z$, because the electron spin quantum number has two values. Therefore, the number of electronic states per unit volume, characterized by n_x , n_y , and n_z lying between n_x and $n_x + \Delta n_x$, n_y and $n_y + \Delta n_y$ and n_z and $n_z + \Delta n_z$, respectively is

$$2\Delta n_x \Delta n_y \Delta n_z / L_x L_y L_z$$

Substituting for (n_x/L_x) , (n_y/L_y) , and (n_z/L_z) from (2.4) in the above expression the number of electronic energy states $d^3 n_s$ per unit volume corresponding to electron momenta between p and $p + dp$ is given by

$$d^3 n_s = (2/h^3) dp_x dp_y dp_z. \quad (2.5)$$

To evaluate the number of states with momenta between p and $p + dp$, the above equation has to be integrated such that the volume element $dp_x dp_y dp_z$ lies between spheres of radius p and $p + dp$ because

$$p_x^2 + p_y^2 + p_z^2 = p^2$$

represents a sphere in the p_x, p_y, p_z space. Since the volume of the p space between spheres of radius p and $p + dp$ is $4\pi p^2 dp$, the number of electronic energy states with momenta between p and $p + dp$ per unit volume is

$$dn_s = (2/h^3)4\pi p^2 dp = (8\pi p^2/h^3)dp, \quad (2.6)$$

An alternate derivation of (2.5) and (2.6), based on the uncertainty relation has been given by Seitz [37].

2.1.3 Distribution Function

The probability $P(E)$ of the occupation of a state of energy $E = p^2/2m_e$ by electrons is given by the *Fermi-Dirac* distribution, viz.

$$P(E) = F_D[(E - E_F)/k_B T], \quad (2.7)$$

where

$$F_D(\Omega) = [1 + \exp \Omega]^{-1},$$

k_B is Boltzmann's constant,
 T is the temperature of the electrons and
 E_F is the Fermi energy.

Therefore from (2.5), (2.6), and (2.7) the number of electrons per unit volume with momenta between \mathbf{p} and $\mathbf{p} + d\mathbf{p}$ is given by

$$d^3 n_e = (2/h^3)F_D[(p^2/2m_e k_B T) - (E_F/k_B T)]dp_x dp_y dp_z. \quad (2.8a)$$

and correspondingly

$$dn_e = (8\pi p^2/h^3)F_D[(p^2/2m_e k_B T) - (E_F/k_B T)]dp, \quad (2.8b)$$

is the number of electrons per unit volume with momentum between \mathbf{p} and $\mathbf{p} + d\mathbf{p}$.

The number of electrons $d^3 n_1$, having momenta between \mathbf{p} and $\mathbf{p} + d\mathbf{p}$, which are incident on the surface (from inside) per unit area per unit time is given by

$$d^3 n_1 = (p_x/m_e)d^3 n_e, \quad (2.8c)$$

where \mathbf{x} is normal to the surface.

If p_t is the magnitude of the transverse component (normal to \mathbf{x}) of the electron momentum,

$$p_t^2 = p_y^2 + p_z^2$$

and $dp_y dp_z$ may be integrated as $2\pi p_t dp_t$, which is the area between two circles of radii p_t and $p_t + dp_t$, respectively. Hence from (2.8c) and (2.8a), one obtains

$$d^2 n_1 = (4\pi/h^3) F_D[(p^2/2m_e k_B T) - (E_F/k_B T)](p_x/m_e) p_t dp_x dp_t.$$

Putting $\varepsilon_x = (p_x^2/2m_e k_B T)$, $\varepsilon_t = (p_t^2/2m_e k_B T)$ and $\varepsilon_F = (E_F/k_B T)$, the above equation may be expressed as:

$$d^2 n_1 = (4\pi m_e k_B^2 T^2 / h^3) F_D(\varepsilon_x + \varepsilon_t - \varepsilon_F) d\varepsilon_x d\varepsilon_t = (A_0 T^2 / e) F_D(\varepsilon_x + \varepsilon_t - \varepsilon_F) d\varepsilon_x d\varepsilon_t \quad (2.9)$$

where $A_0 = (4\pi e m_e k_B^2 / h^3) = 120 \text{ A/cm}^2 \text{K}^2$ and $-e$ is the electronic charge.

In the above equation, ε_x and ε_t represent the normalized normal and transverse kinetic energies on account of the normal (p_x) and transverse (p_t) components of the electron momentum in the metal. The parameter $\varepsilon_x + \varepsilon_t$ represents the total normalized electron energy, while ε_F is the normalized Fermi energy. The parameters ε_x , ε_t , and ε_F are all positive.

2.1.4 Fermi Energy

Putting $E = (p^2/2m_e)$ in (2.8b) one obtains

$$dn_e = (8\pi/h^3)(2m_e)^{1/2} F_D[(E - E_F)/k_B T] E^{1/2} dE$$

or

$$n_e = (8\pi/h^3)(2m_e)^{1/2} \int_0^\infty E^{1/2} F_D[(E - E_F)/k_B T] dE, \quad (2.10)$$

where n_e is the number of electrons per unit volume, i.e., the electron density.

The above equation can be used to evaluate the *Fermi energy* E_F , corresponding to a given electron density n_e and the temperature T .

A simple expression for Fermi energy E_{F0} can be obtained at the temperature 0 K, corresponding to

$$F_D = 0 \quad \text{for } E > E_{F0}$$

and

$$F_D = 1 \quad \text{for } E < E_{F0}.$$

Thus, the electron density

$$n_e = \int_0^{E_{F0}} (8\pi/h^3)(2m_e)^{1/2} E^{1/2} dE,$$

which leads to

$$E_{F0} = (h^2/8m_e)(3n_e/8\pi)^{2/3}. \quad (2.11)$$

Using (2.10), one may obtain [37] an approximate expression for the Fermi energy E_F corresponding to an electron density n_e and finite temperature T , as

$$\begin{aligned} E_F &\approx E_{F0}[1 - (\pi^2/8)(k_B T/E_{F0})]^{2/3} \\ &\approx E_{F0}[1 - (\pi^2/12)(k_B T/E_{F0})]. \end{aligned} \quad (2.12)$$

where E_{F0} is given by (2.11) and is much larger than $k_B T$.

2.2 Basic Concepts of Electron Emission

2.2.1 Potential Energy of an Electron Near the Plane Surface of a Metal

The attractive force on an electron, with charge $-e$ at a distance x from a plane metallic surface is the same as that exerted by a particle with an equal and opposite charge at the same distance from the surface on the other side; it may be noted that the two charges and their positions ensure zero electric potential on the surface. Hence the force, termed as image force on the electron $F_i(x)$ is given by

$$F_i(x) = -e^2/(x+x)^2 = -e^2/4x^2.$$

and the associated potential energy $V_i(x)$ is given by

$$V_i(x) = - \int_{\infty}^x F_i(x) dx = -e^2/4x.$$

According to the free electron theory of metals, the potential energy of an electron inside a metal is $-W_a$; to ensure a uniform electric potential ($-V_0/e$) on the surface (or a potential energy $V_0 - W_a$ in the metal) and to take into account the applied electric field F and the image force, the potential energy $V(x)$ of an electron ($x > 0$) is given by [37]

$$V(x) = V_0 - eFx - e^2/[(e^2/W_a) + 4x]. \quad (2.13a)$$

Neglecting the term (e^2/W_a) in (2.13a)

$$V(x) = V_0 - eFx - e^2/4x. \quad (2.13b)$$

The position x_m and magnitude V_m of the maximum potential energy is given by putting $dV/dx = 0$ and using (2.13b); the condition $d^2V/dx^2 < 0$ at $x = x_m$ (for a maximum) can be easily verified. Thus,

$$x_m = (e/F)^{1/2}/2$$

and

$$V_m = V_0 - (e^3F)^{1/2}. \quad (2.14)$$

It is also seen that $(e^2/W_a) \ll x_m$ for usual values of the parameters and hence (2.13b) is valid around $x = x_m$. Thus, the effective height of the potential energy barrier W_a' is less than W_a by $(e^3F)^{1/2}$ in the presence of an electric field F . Thus

$$W_a' = V_m - V(x=0) = W_a - (e^3F)^{1/2} \quad (2.15)$$

The additional electron emission due to the reduction in the potential energy surface barrier is known as Schottky Emission [36]. The electron potential energy model, represented by (2.13a) is too cumbersome, to be used conveniently for the study of electron emission. Hence, one may adopt a simpler model represented by Fig. 2.1f, g, which incorporates the essential feature of (2.13a) viz. the reduction of the surface energy barrier. The potential energy models, adopted for the evaluation of the transmission coefficient of an electron through the surface in different papers are illustrated in Fig. 2.1a–g and represented analytically by (2.16a) to (2.16g) in Table 2.1. From classical considerations, the transmission coefficient is unity when the normal electron energy due to the velocity component normal to the surface exceeds W_a and is zero otherwise. However, from wave mechanical considerations, discussed later the results are substantially different. The figures correspond to different regions, (characterized in Table 2.1) and negatively charged surface except Fig. 2.1, which corresponds to a positively charged surface.

Here W_a is the height of the surface potential energy barrier, F is the electric field outside the metallic surface, x is the distance normal to the surface, $(-e^2/4x)$ is the potential energy of the electron due to the image force and $W_a' [= W_a - (e^3F)^{1/2}]$ is the reduced height of the surface potential energy barrier on account of the *Schottky* effect (2.15). The three region model incorporates a field free region, which is physically realistic. If Region-III consists of the anode $V(x) = -W_a'$ in region III.

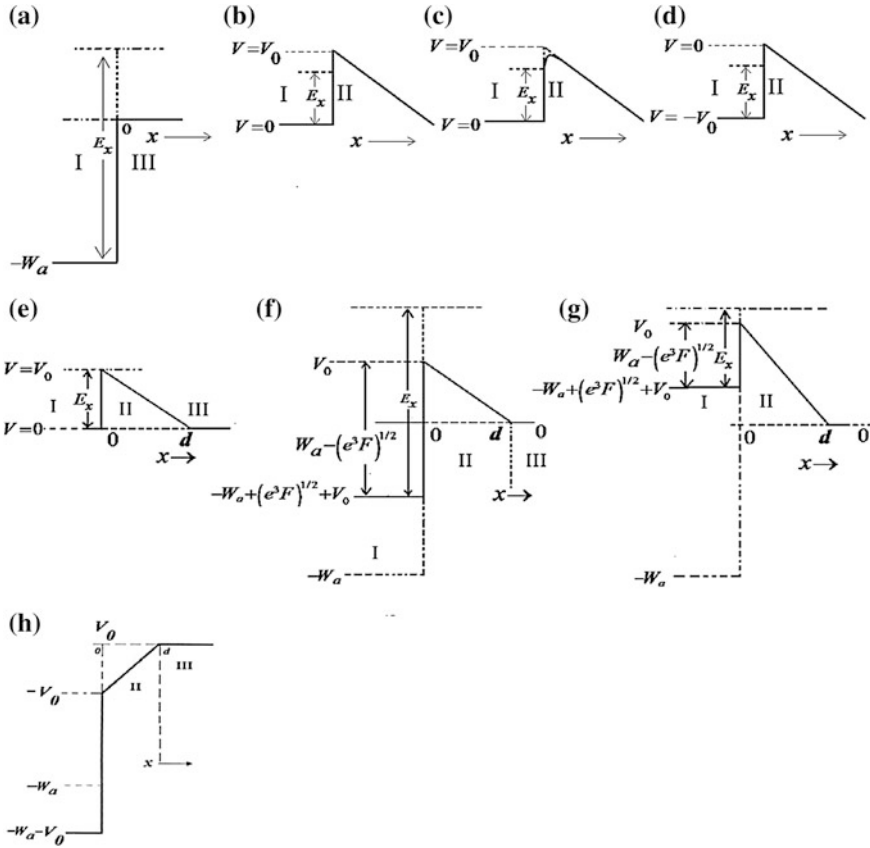


Fig. 2.1 Potential energy of an electron near the surface of a metallic plate. The labels are as follows: **a** Uncharged surface, **b** two region Fowler's model [15] (negatively charged), **c** two region Schottky/Nordheim [32] model (negatively charged), **d** two region Forbes and Deane [12] model (negatively charged) **e** three region model by Sodha et al. [40] (negatively charged), **f** negatively charged surface with $V_0 < W_a$ and **g** negatively charged surface with $V_0 > W_a$; **f** and **g** correspond to the present three region model and **h** positively charged surface ($V_0 < 0$) (after Agarwal et al. [1]; curtesy authors and publishers NRC Press)

2.2.2 Transmission Coefficient Across Metallic Plane Surfaces: Uncharged Surface

The transmission coefficient of an electron through the surface can be evaluated from matching the solution (ψ and $d\psi/dx$) of *Schrödinger's* equation at the interface of the two regions.

The derivation of an expression for the transmission coefficient $D(E_x)$ corresponding to an uncharged surface with electron potential energy, described by

Table 2.1 Models of potential energy of an electron near a negatively charged plane metallic surface ($x = 0$)

Fig. 2.1a	Region-I	$V(x) = -W_a$	$x < 0$	
Simple model (uncharged)	Region-II	$V(x) = 0$	$x > 0$	(2.16a)
Fig. 2.1b	Region-I	$V(x) = 0$	$x < 0$	
Fowler and Nordheim [15]	Region-II	$V(x) = V_0 - eF(x)$	$x > 0$	(2.16b)
Fig. 2.1c	Region-I	$V(x) = -W_a$	$x < 0$	
Forbes and Deane [12]	Region-II	$V(x) = -eF(x)$	$x > 0$	(2.16c)
Fig. 2.1d	Region-I	$V(x) = 0$	$x < 0$	
Schottky/ Nordheim [32]	Region-II	$V(x) = V_0 - eF(x) - (e^2/4x)$	$x > 0$	(2.16d)
Fig. 2.1e	Region-I	$V(x) = 0$	$x < 0$	
Sodha and Dixit [40]	Region-II	$V(x) = V_0 - eF(x)$	$0 < x < d(= V_0/eF)$	
	Region-III	$V(x) = 0$	$x > d$	(2.16e)
Fig. 2.1f ($V_0 > W_a$)	Region-I	$V(x) = V_0 - W_a'$	$x < 0$	
Fig. 2.1g ($V_0 < W_a$)	Region-II	$V(x) = V_0 - eF(x)$	$0 < x < d(= V_0/eF)$	
(Three region model)	Region-III	$V(x) = 0$	$x > d$	(2.16f, g)
Fig. 2.1h ($V_0 < 0$)	Region-I	$V(x) = V_0 - W_a$	$x < 0$	(2.16h)
	Region-II	$V(x) = V_0 - V_0(x/d)$	$x > 0$	
	Region-III	$V(x) = 0$	$x > d$	

After Agarwal et al. [1]; courtesy authors and publishers NRC Press

(2.16a) is given in many books on Quantum Mechanics (e.g., [17]). Thus, the transmission coefficient $D_0(E_x)$ is given by

$$\begin{aligned}
 D_0(E_x) &= 4E_x^{1/2}(E_x - W_a)^{1/2} / [E_x^{1/2} + (E_x - W_a)^{1/2}]^2 \\
 &= 4\varepsilon_x^{1/2}(\varepsilon_x - w_a)^{1/2} / [\varepsilon_x^{1/2} + (\varepsilon_x - w_a)^{1/2}]^2,
 \end{aligned} \tag{2.17}$$

where

$$\varepsilon_x = E_x / k_B T,$$

$$w_a = W_a / k_B T$$

and E_x is the normal component of kinetic energy of the electron in the metal.

To a first approximation (2.17) is valid for negatively charged surfaces, when W_a is replaced by $W_a - e^{3/2}F^{1/2}$ (2.15) and E_x is significantly larger than W_a . For a positively charged surface ($V_0 < 0$) (2.17) is an approximation when W_a is replaced by $W_a - V_0$; the surface is then charged to an electric potential $(-V_0/e)$.

2.2.2.1 Negatively Charged Surface (After Agarwal et al. [1])

Referring to Fig. 2.1f, g, one notices that from wave mechanical considerations the transmission coefficient, $D(E_x)$ is also finite for $W_a - V_0 - e^{3/2}F^{1/2} < E_x < W_a - e^{3/2}F^{1/2}$, when $W_a > V_0$ and $0 < E_x < W_a - e^{3/2}F^{1/2}$ for $W_a < V_0$ on account of tunneling, where V_0 is the potential energy of electrons at the surface; this accounts for the electric field emission. A critique of the theories of electric field emission has been given by [12, 40]. Little attention has however been given to $D(E_x)$ (for a negatively charged surface) for electrons with $E_x > W_a - e^{3/2}F^{1/2}$, which are responsible for thermionic and photoelectric emission. This may be due to the electric field emission studies being mainly limited to low temperatures.

The frequently used [15] model, which is the basis of the famous *Fowler–Nordheim equation* for the electric field emission, is illustrated in Fig. 2.1d. This model ignores the fact that $V(x) = (-W_a + V_0 + e^{3/2}F^{1/2})$ in Region-I and also the existence of Region-III where $V = 0$. The vast amount of work on two region models, corresponding to Fig. 2.1d has been critically reviewed by Forbes and Deane [12]. Some models (Fig. 2.1e) have taken into account (e.g., [40] Region-III but have ignored the fact that in Region-I, $V(x) = (-W_a + V_0 + e^{3/2}F^{1/2})$. Nordheim [32] has used a model similar to that in Fig. 2.1b except that in Region-II, the potential energy takes into account the image force (Fig. 2.1d). Because of ignoring the surface energy barrier in these models, the corresponding evaluated transmission coefficients and the electron emission currents, lack a sound foundation.

In what follows an expression for $D(E_x)$ corresponding to a negatively charged surface has been derived and the dependence of $D(E_x)$ on electron energy, electric field, and height of the surface energy barrier has been graphically illustrated; it is seen that $D(E_x)$ is an increasing function of E_x and hence the thermionic and photoelectric currents should also increase with increasing field F . The dependence of thermionic and photoelectric current density on the electric field and the height of the surface energy barrier has also been investigated and the results have been graphically illustrated in later sections. For the sake of completeness, the currents on account of the electric field emission and light-induced field emission as a function of W_a and F have also been evaluated; the earlier studies pertained to low temperatures.

It is seen that the electric field significantly enhances the transmission coefficient of an electron across the surface and hence for the evaluation of the electron emission from a metal an appropriate expression for $D(E_x)$, (derived herein), should be used for negatively charged surfaces. The electron emission, corresponding to a positively charged surface is also briefly discussed later for the sake of completeness.

2.2.2.2 Expression for $D(E_x)$

The potential energy of an electron inside and outside a negatively charged plane metallic surface may be modeled by (2.16f, g).

The time independent Schrödinger equation is

$$\nabla^2 \psi(x, y, z) + \frac{8\pi^2 m_e}{h^2} [E - V(x)] \psi(x, y, z) = 0. \quad (2.18)$$

Using the method of separation of variables by substituting $\psi = \psi_x(x)\psi_y(y)\psi_z(z)$, the above equation reduces to

$$\begin{aligned} &(\psi_x)^{-1} (d^2 \psi_x / dx^2) + (\psi_y)^{-1} (d^2 \psi_y / dy^2) \\ &+ (\psi_z)^{-1} (d^2 \psi_z / dz^2) + (8\pi^2 m_e / h^2) [E - V(x)] = 0 \end{aligned} \quad (2.19)$$

The first and fourth terms are functions of x only, while the second and third terms are respectively functions of only y and z . Hence, one can write

$$(\psi_y)^{-1} (d^2 \psi_y / dy^2) = -k_y^2 \quad \text{and} \quad (\psi_z)^{-1} (d^2 \psi_z / dz^2) = -k_z^2, \quad (2.20)$$

where k_y and k_z are recognizable as the components of the wave vector \mathbf{k} , associated with the wave function ψ . Use of the relation $\mathbf{k} = (2\pi/h)\mathbf{p}$, (2.3a, 2.3b) and (2.4) leads to

$$d^2 \psi_x / dx^2 + (8\pi^2 m_e / h^2) [E'_x - V(x)] \psi_x = 0, \quad (2.21)$$

where \mathbf{p} is the electron momentum and $E'_x = E - (p_y^2 / 2m_e) - (p_z^2 / 2m_e)$ represents the difference between the total energy and the kinetic energy due to the transverse components p_y and p_z of the momentum \mathbf{p} .

If $E_x = (p_x^2 / 2m_e)$ denotes the normal kinetic energy of the electron inside $[V(x) = -W_a + (e^3 F)^{1/2} + V_0]$ the metal on account of the normal (i.e., x) component of the momentum, one can write

$$E'_x = E_x - W_a + (e^3 F)^{1/2} + V_0. \quad (2.22)$$

Thus, (2.21) can be expressed as

$$d^2 \psi_x / dx^2 + (8\pi^2 m_e / h^2) [E_x - W_a + (e^3 F)^{1/2} + V_0 - V(x)] \psi_x = 0, \quad (2.23)$$

From (2.16f, g) and (2.23), one obtains the following set of dimensionless equations for the three-region model

$$\frac{d^2 \psi_x}{d\xi^2} + \varepsilon_x \psi_x = 0, \quad \xi < 0 \quad \text{Region-I} \quad (2.24a)$$

$$\frac{d^2 \psi_x}{d\xi^2} + [\varepsilon_x - w_a + \alpha f^{1/2} + f\xi] \psi_x = 0, \quad 0 < \xi < \xi_0 \quad \text{Region-II} \quad (2.24b)$$

and

$$\frac{d^2 \psi_x}{d\xi^2} + [\varepsilon_x + v_0 - w_a + \alpha f^{1/2}] \psi_x = 0, \quad \xi > \xi_0 \quad \text{Region-III} \quad (2.24c)$$

where $\varepsilon_x = E_x/k_B T$, $v_0 = V_0/k_B T = eFd/k_B T$, $w_a = W_a/k_B T$, $f = heF/(\pi k_B T \sqrt{8m_e k_B T})$ is the dimensionless electric field strength in Region-II,

$$\alpha = (8\pi^2 m_e / h^2 k_B T)^{1/4} e,$$

$$\xi = (\pi \sqrt{8m_e k_B T} / h) x,$$

$$\xi_0 = (\pi \sqrt{8m_e k_B T} / h) d, (V_0 / eF) = v_0 / f \text{ and } T \text{ is the temperature of the metal.}$$

The solution of (2.24a), (2.24b), and (2.24c) may be written as

$$\psi_x(\xi) = A_1 \exp(ik_1 \xi) + A_2 \exp(-ik_1 \xi), \quad \text{Region-I} \quad (2.25a)$$

$$\begin{aligned} \psi_x(\xi) = & B_1 Ai[-(\varepsilon_x - w_a + \alpha f^{1/2} + f\xi)/f^{2/3}] \\ & + B_2 Bi[-(\varepsilon_x - w_a + \alpha f^{1/2} + f\xi)/f^{2/3}] \quad \text{Region-II} \end{aligned} \quad (2.25b)$$

and

$$\psi_x(\xi) = C_1 \exp(ik_3 \xi), \quad \text{Region-III} \quad (2.25c)$$

where Ai and Bi are Airy functions,

$$k_1^2 = \varepsilon_x \quad \text{and} \quad k_3^2 = [\varepsilon_x + v_0 - w_a + \alpha f^{1/2}].$$

The constants a_1 , a_2 , b_1 , b_2 , and c_1 are related by the fact that the wave function and its derivative is continuous at the boundaries. viz., at $\xi = 0$ and $\xi = \xi_0$.

Thus at $\xi = 0$

$$a_1 + a_2 = b_1 l_2 + b_2 m_2, \quad (2.26a)$$

and

$$ik_1 a_1 - ik_1 a_2 = -b_1 l'_2 f^{1/3} - b_2 m'_2 f^{1/3}. \quad (2.26b)$$

and at $\xi = \xi_0$

$$b_1 l_1 + b_2 m_1 = C_1 \exp(ik_3 \xi_0) \quad (2.26c)$$

and

$$-b_1 l'_1 f^{1/3} - b_2 m'_1 f^{1/3} = ik_3 c_1 \exp(ik_3 \xi_0), \quad (2.26d)$$

where

$$\begin{aligned}
l_1 &= Ai[-(\varepsilon_x + v_0 - w_a + \alpha f^{1/2})/f^{2/3}], \quad l'_1 = Ai'[-(\varepsilon_x + v_0 - w_a + \alpha f^{1/2})/f^{2/3}] \\
l_2 &= Ai[-(\varepsilon_x - w_a + \alpha f^{1/2})/f^{2/3}], \quad l'_2 = Ai'[-(\varepsilon_x - w_a + \alpha f^{1/2})/f^{2/3}], \\
m_1 &= Bi[-(\varepsilon_x + v_0 - w_a + \alpha f^{1/2})/f^{2/3}], \quad m'_1 = Bi'[-(\varepsilon_x + v_0 - w_a + \alpha f^{1/2})/f^{2/3}], \\
m'_1 &= Bi'[-(\varepsilon_x + v_0 - w_a + \alpha f^{1/2})/f^{2/3}] \\
m_2 &= Bi[-(\varepsilon_x - w_a + \alpha f^{1/2})/f^{2/3}] \quad \text{and} \\
m'_2 &= Bi'[-(\varepsilon_x - w_a + \alpha f^{1/2})/f^{2/3}].
\end{aligned}$$

From (2.26a), (2.26b), (2.26c), and (2.26d), one obtains

$$\frac{c_1}{a_1} = \frac{2ik_1\delta_5 f^{1/3} \exp(-ik_3\xi_0)}{\{k_1k_3\delta_1 + \delta_2 f^{2/3}\} + i(k_1\delta_4 + k_3\delta_3)f^{1/3}} \quad (2.27)$$

where $(m_1l_2 - l_1m_2) = \delta_1$, $(m'_1l'_2 - m'_2l'_1) = \delta_2$, $(m_1l'_2 - m'_2l_1) = \delta_3$, $(m_2l'_1 - m'_1l_2) = \delta_4$ and $(m_1l'_1 - m'_1l_1) = \delta_5$.

From (2.27), one obtains

$$\frac{c_1c_1^*}{a_1a_1^*} = \frac{4k_1^2\delta_5^2 f^{2/3}}{\{k_1k_3\delta_1 + \delta_2 f^{2/3}\}^2 + (k_1\delta_4 + k_3\delta_3)^2 f^{2/3}} \quad (2.28)$$

Further, the probability current density normal to the surface is given by

$$j_x = \frac{i\hbar}{4\pi m_e} \left(\psi_x \frac{\partial}{\partial \xi} \psi_x^* - \psi_x^* \frac{\partial}{\partial \xi} \psi_x \right) \quad (2.29)$$

Hence, the probability current density in Region-I is given by

$$(j_x)_I = \frac{k_1\hbar}{2\pi m_e} [a_1^*a_1 - a_2^*a_2]$$

In the above expression, the first term on the right-hand side represents the incident current while the second term represents the reflected current. Thus, the incident current density in Region-I is given by

$$(j_x)_i = \frac{k_1\hbar}{2\pi m_e} a_1^*a_1 \quad (2.30)$$

Similarly, the transmitted current density in Region-III is given by

$$(j_x)_t = \frac{k_3\hbar}{2\pi m_e} c_1c_1^* \quad (2.31)$$

Hence, the transmission coefficient D across the potential energy barrier at the surface is given by

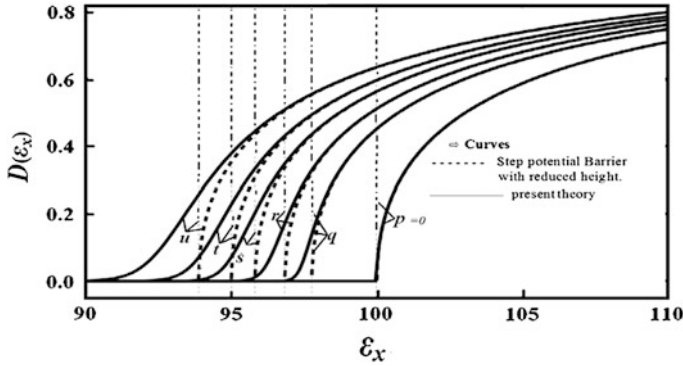


Fig. 2.2 Dependence of Transmission-coefficient $D(\varepsilon_x)$ on ε_x for the parameters $T = 1000$ K, $w_a = 100$ and $v_0 = 10^4$. The different values of field strength has been shown on the graph by letters; p, q, r, s, t and u correspond to $f = 0, 0.2, 0.4, 0.7, 1.0$ and 1.5 respectively. The portion of the curves corresponding to left and right-hand side of the vertical lines refer to field emission and thermionic emission respectively (after Agarwal et al. [1]; curtesy authors and publishers NRC Press)

$$D = \frac{(j_x)_t}{(j_x)_i} = \frac{k_3 c_1 c_1^*}{k_1 a_1 a_1^*} \quad (2.32)$$

which using (2.28) can be reduced to

$$D(\varepsilon_x) = \frac{4k_1 k_3 \delta_5^2 f^{2/3}}{\{k_1 k_3 \delta_1 + \delta_2 f^{2/3}\}^2 + (k_1 \delta_4 + k_3 \delta_3)^2 f^{2/3}}, \quad (2.32a)$$

According to Fowler [13], a fraction of electrons get their normal energy enhanced by an amount $h\nu$, when the surface is irradiated by light of frequency ν . Hence the transmission coefficient $D_{ph}(\varepsilon_x)$ of such electrons can be obtained by substituting $(\varepsilon_x + \varepsilon_\nu)$ for ε_x in (2.32a), where $\varepsilon_\nu = (h\nu/k_B T)$. Thus

$$D_{ph}(\varepsilon_x) = D(\varepsilon_x + \varepsilon_\nu). \quad (2.32b)$$

Equation (2.32a) is also valid in the case of positively charged surfaces when one substitutes $(-v_0)$ for v_0 and $-f$ for f in the inherent coefficients in the final expression for $D(\varepsilon_x)$.

The set of Fig. 2.2 and 2.3 illustrate the dependence of transmission coefficient $[D(\varepsilon_x)]$ on the normal energy of electrons ε_x , as a function of dimensionless field strength (f) (Fig. 2.2) and the potential energy barrier height (w_a) (Fig. 2.3). It is seen that $D(\varepsilon_x)$ increases monotonically with increasing ε_x and f .

The straight vertical dashed lines are indicative of the effective surface energy barrier ($w_a - \alpha f^{1/2}$), so that the points to the left of these lines contribute to the electric field emission while those to the right contribute to thermionic emission; the broken curves correspond to transmission coefficient for step potential barrier with reduced barrier height $D_0(\varepsilon_x)$. It is interesting to notice that contribution of the

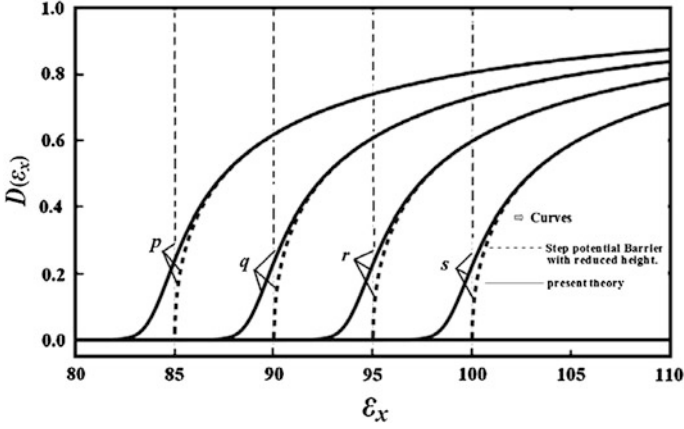


Fig. 2.3 Dependence of Transmission-coefficient $D(\epsilon_x)$ as a function of ϵ_x for the parameters $T = 1000$ K, $f = 1$ and $v_0 = 10^4$. The different values of w_a parameter have been shown on the graph by letters. The letters p , q , r and s refer to $w_a = 90, 95, 100$ and 105 respectively (after Agarwal et al. [1]; curtsey authors and publishers NRC Press)

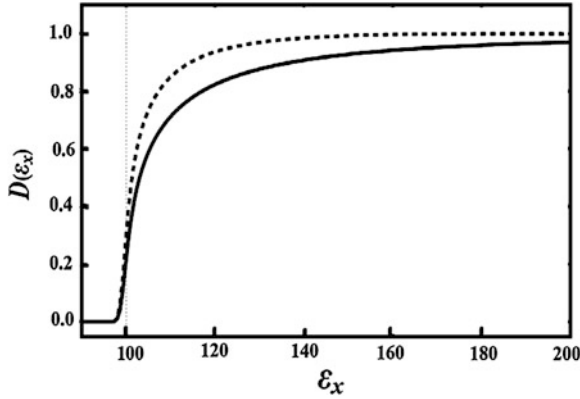


Fig. 2.4 Dependence of $D(\epsilon_x)$ on ϵ_x for the Case-I as stated in the text, for the parameters $T = 1000$ K, $f = 1$, $w_a = 120$ and $v_0 = 1.0 \times 10^4$; here the role of image force is ignored. The *solid curve* corresponds to the present three region model while the *broken curve* refers to Forbes and Deane's approach (after Agarwal et al. [1]; curtsey authors and publishers NRC Press)

field emission and departure of $D(\epsilon_x)$ from $D_0(\epsilon_x)$ increase with increasing f . The figure also reflects the fact that $D_0(\epsilon_x)$ is only meaningful for $\epsilon_x > (w_a - \alpha f^{1/2})$. Figure 2.3 indicates that $D(\epsilon_x)$ decreases with increasing potential energy barrier height (w_a). It is seen that the surface potential energy v_0 has no significant effect on the energy dependence of $D(\epsilon_x)$. It is seen from Fig. 2.4 that the expression due to Forbes and Dean [12], based on the two region model overestimates the transmission coefficient except for very high and low values of ϵ_x compared to w_a .

2.2.3 Thermionic and Electric Field Emission of Electrons from a Plane Surface

2.2.3.1 Negatively Charged Surface

From classical considerations electrons hitting the surface with normal energy $\varepsilon_x > (w_a - \alpha f^{1/2})$ have a unit probability of crossing the surface or of emission; such an emission is known as thermionic emission. However, wave mechanical considerations, outlined before lead to a probability of emission $D(\varepsilon_x)$, given by (2.32a). The number of electrons hitting the surface per unit area per unit time and having normal energy between ε_x and $\varepsilon_x + d\varepsilon_x$ and transverse energy between ε_t and $\varepsilon_t + d\varepsilon_t$ is

$$d^2n_1 = (A_0/e)T^2 F_D(\varepsilon_x + \varepsilon_t - \varepsilon_F) d\varepsilon_x d\varepsilon_t, \quad (2.9)$$

Hence, the number n_{th} of electrons emitted from the surface per unit area per unit time and the corresponding electric current J_{th} is given by

$$\begin{aligned} J_{th} &= -en_{th} = -e \int_{\varepsilon_x=(w_a-\alpha f^{1/2})}^{\infty} \int_{\varepsilon_t=0}^{\infty} D(\varepsilon_x) d^2n_1 \\ &= -A_0 T^2 \int_{(w_a-\alpha f^{1/2})}^{\infty} \int_0^{\infty} D(\varepsilon_x) \cdot F_D(\varepsilon_x + \varepsilon_t - \varepsilon_F) d\varepsilon_x d\varepsilon_t. \end{aligned} \quad (2.33)$$

For electrons of interest to thermionic emission, $\varepsilon_x > (w_a - \alpha f^{1/2})$,

$$\eta = (\varepsilon_x + \varepsilon_t - \varepsilon_F) > (w_a - \varepsilon_F + \varepsilon_t) - \alpha f^{1/2}$$

$[\approx \varphi + \varepsilon_t - \alpha f^{1/2}]$ is much larger than unity, where $\varphi = (w_a - \varepsilon_F) = (W_a - E_F)/k_B T = \Phi/k_B T$, and Φ is known as the work function of the metal. Hence $F_D(\eta) \rightarrow \exp(-\eta)$ and (2.9) simplifies to

$$d^2n_1 = (A_0/e)T^2 \exp(-\varepsilon_x - \varepsilon_t + \varepsilon_F) d\varepsilon_x d\varepsilon_t, \quad (2.9a)$$

Thus (2.33) reduces to

$$\begin{aligned} J_{th} &= -en_{th} = -e(A_0 T^2/e) \int_{(w_a-\alpha f^{1/2})}^{\infty} \int_0^{\infty} D(\varepsilon_x) \cdot \exp(-\varepsilon_x - \varepsilon_t + \varepsilon_F) d\varepsilon_x d\varepsilon_t \\ &= -A_0 T^2 \int_{(w_a-\alpha f^{1/2})}^{\infty} D(\varepsilon_x) \cdot \exp(-\varepsilon_x + \varepsilon_F) d\varepsilon_x \end{aligned} \quad (2.34a)$$

In most of investigations on thermionic emission, the transmission coefficient is assumed to be unity; as evident from Figs. 2.2, 2.3 and similar calculations for other parameters this is indeed a poor approximation.

However, putting $D(\varepsilon_x) = 1$ (2.34a) reduces to

$$J'_{\text{th0}} = -A_0 T^2 \exp(-w_a + \alpha f^{1/2} + \varepsilon_F) = -A_0 T^2 \exp(-\varphi + \alpha f^{1/2}) \quad (2.34b)$$

and

$$J_{\text{th}}/J'_{\text{th0}} = \exp(\varphi - \alpha f^{1/2}) \int_{(w_a - \alpha f^{1/2})}^{\infty} D(\varepsilon_x) \exp(-\varepsilon_x + \varepsilon_F) d\varepsilon_x \quad (2.34c)$$

For an uncharged surface $f = 0$ and if $D(\varepsilon_x) = 1$ (2.34b) reduces to

$$J_{\text{th0}} = -A_0 T^2 \exp(-\varphi) = -A_0 T^2 \exp(-\Phi/k_B T). \quad (2.35a)$$

The above equation is known as *Richardson Dushman* equation.

For metals, as well as semiconductors the experimental data conforms to the relation

$$J_{\text{th0}} = -A T^2 \exp(-\Phi/k_B T), \quad (2.35b)$$

where the constant A is known as *Richardson's Constant* and is in general different from A_0 .

For an uncharged surface and $D(\varepsilon_x) = 1$, the mean energy ε_{th0} of the emitted electrons at the surface is given by

$$\varepsilon_{\text{th0}} = \int_{w_a}^{\infty} \int_0^{\infty} (\varepsilon_x + \varepsilon_t - w_a) d^2 n_1 \bigg/ \int_{w_a}^{\infty} \int_0^{\infty} d^2 n_1$$

Using (2.9) and putting $\varepsilon'_x = \varepsilon_x - w_a$ and $\varepsilon' = \varepsilon'_x + \varepsilon_t$

$$\begin{aligned} \varepsilon_{\text{th0}} &= \int_0^{\infty} \int_0^{\infty} (\varepsilon'_x + \varepsilon_t) \exp(-\varepsilon'_x - \varepsilon'_t) d\varepsilon'_x d\varepsilon'_t \bigg/ \int_0^{\infty} \int_0^{\infty} \exp(-\varepsilon'_x - \varepsilon'_t) d\varepsilon'_x d\varepsilon'_t \\ &= \int_0^{\infty} (\varepsilon'^2) \exp(-\varepsilon') d\varepsilon' \bigg/ \int_0^{\infty} \varepsilon' \exp(-\varepsilon') d\varepsilon' = 2 \quad (\text{just outside the surface}) \end{aligned} \quad (2.36a)$$

In writing the above equation, the following identity has been used

$$\int_0^{\infty} \int_0^{\infty} f(x_1 + x_2) dx_1 dx_2 = \int_{x_0}^{\infty} x f(x) dx \quad (2.37)$$

$$x_1 + x_2 > x_0$$

For a negatively charged surface at a potential $(-V_0/e)$, the mean electron energy far away from the surface is

$$\varepsilon_{\text{th}} = 2 + v_0. \quad (2.36b)$$

The values of *Richardson's Constant* for different metals are different from one another as well as from A_0 . The reasons for departure of A from A_0 , as given by Seitz [37] are as follows:

- I. The concept of effective mass of an electron is phenomenological; putting effective mass equal to free electronic mass is another approximation.
- II. The interaction of electrons (mutual and with ions) in the metals has been neglected.
- III. The relation $E = (p_x^2 + p_y^2 + p_z^2)/2 m_e$ is at best an approximation, within the metal.
- IV. The assumption of a perfectly plane surface is idealistic.
- V. The coefficient of transmission from the surface for the electrons with $(p_x^2/2m) > W_a - (e^3 F)^{1/2}$ has been assumed to be unity [$D(\varepsilon_x) = 1$].
- VI. The temperature dependence of Φ has been neglected. If one assumes $\Phi = \Phi_0 + \Phi_1 T$, substitution for Φ as above in (2.3b) leads to (2.3c) with $A = A_0 \exp(-\Phi_1/k_B)$. This explains A being larger or smaller than A_0 , depending on the sign of Φ_1 .

The work function Φ and other parameters for some materials has been listed in Table 2.2.

2.2.3.2 Electric Field Emission

As discussed before electrons with $\varepsilon_x < (w_a - \alpha f^{1/2})$ have a finite probability $D(\varepsilon_x)$ of tunneling through the modified surface energy barrier and thus contributing to electron emission, known as electric field emission. Hence proceeding as in the derivation of (2.34a) the field emission current density is given by

$$J_{\text{fe}} = -e \int_0^{w_a - \alpha f^{1/2}} \int_0^\infty D(\varepsilon_x) d^2 n_1 = -A_0 T^2 \int_0^{(w_a - \alpha f^{1/2})} D(\varepsilon_x) \ln[1 + \exp(-\varepsilon_x + \varepsilon_F)] d\varepsilon_x$$

for $v_0 > w_a$

$$(2.38a)$$

and

$$J_{\text{fe}} = -A_0 T^2 \int_{w_a - \alpha f^{1/2} - v_0}^{(w_a - \alpha f^{1/2})} D(\varepsilon_x) \ln[1 + \exp(-\varepsilon_x + \varepsilon_F)] d\varepsilon_x \quad \text{for } v_0 < w_a \quad (2.38b)$$

Table 2.2 Electron emission data

S. No.	Materials	E_F (eV)	W_a (eV)	Φ (eV)	A ($\text{Acm}^{-2}\text{K}^{-2}$)
<i>A. Metals</i>					
1	Li	4.74	7.67	2.93	
2	Na	3.24	5.60	2.36	
3	K	2.12	4.41	2.29	
4	Rb	1.85	4.11	2.26	
5	Cs	1.59	3.54	1.95	160
6	Cu	7.00	12.1–11.53	5.10–4.48	
7	Ag	5.49	10.23–10.01	4.74–4.52	
8	Au	5.53	11.0–10.84	5.47–5.31	
9	Be	14.3	19.28	4.98	
10	Mg	7.08	10.74	3.66	
11	Ca	4.69	7.56	2.87	
12	Sr	3.93	6.42	2.59	
13	Ba	3.64	6.16	2.52	60
14	Nb	5.32	9.27– 9.84	3.95–4.87	
15	Fe	11.1	15.77– 5.91	4.67–4.81	
16	Mn	10.9	15.0	4.1	
17	Zn	9.47	13.10–14.37	3.63–4.9	
18	Cd	7.47	11.55	4.08	
19	Hg	7.13	11.60	4.47	
20	Al	11.7	15.76–15.96	4.06–4.26	
21	Ga	10.4	14.72	4.32	
22	In	8.63	12.72	4.09	
23	Tl	8.15	11.99	3.84	
24	Sn	10.2	14.62	4.42	
25	Pb	9.47	13.72	4.25	
26	Bi	9.9	14.24	4.34	
27	Sb	10.9	15.45–15.6	4.55–4.7	
28	Mo			4.36–4.95	55
29	Ni			5.04–5.35	60
30	Ta			4.0–4.8	60
31	W			4.45–5.22	80
32	Pt			5.22–5.93	170
33	Th			3.4	70
34	Zr			4.05	330
35	Hf			3.9	14.5
36	Pd			5.22–5.6	60
37	Ca			2.86	2.6
38	Sr			2.67	0.14
39	Ba			2.45	16
<i>B. Borides</i>					
40	La			2.66	29
41	Ce			2.58	3.6
42	Th			2.92	0.5

(continued)

Table 2.2 (continued)

S. No.	Materials	E_F (eV)	W_a (eV)	Φ (eV)	A (Acm ⁻² K ⁻²)
<i>C. Carbides</i>					
43	Ta			3.14	0.3
44	Ti			3.35	25
45	Zr			2.18	0.3
46	Th			3.5	550
47	Ur			3.3	40
48	Th on W			2.63	3.0
49	Th on Mo			2.58	1.5
50	Zr on W			3.14	5.0
51	La, Ce on W			2.71	8.0
52	Cs on W			1.36	3.2
53	O on W			9.2	5×10^{11}
54	Cs on O on W			0.72	0.003
<i>D.Mono molecular films</i>					
55	Ba on W			1.56	1.5
56	Ba on O on W			1.34	0.18
57	Ice			8.7	

Note The values for E_F , W_a and Φ for materials 1–36 have been taken from Lide [25]

The values of A for materials 5, 13, 28–36 and 48–56 are from Fowler [14]

The values of Φ for materials 48–56 are from Fowler [14]

The values of A and Φ for materials 37–47 are from Jenkins and Trodder [22]

The value of Φ for ice is an indirect reference from Klumov et al. [24]

The limits can be appreciated by looking at Fig. (2.1f, g).

2.2.3.3 Numerical Results and Discussion

For an appreciation of the results computations were made, corresponding to the parameters $T = 1000$ K when

$$w_a = 38.64(W_a \text{ in eV}), f = 4.7 \times 10^{-6}(F \text{ in V/cm}) \text{ and } v_0 = 38.64(\eta_0 \text{ in eV});$$

η_0 is surface potential energy of an electron. The dependence of the field emission (J_{fe}/J_{th0}) and thermionic (J_{th}/J_{th0}) emission currents on the dimensionless field strength (f) for different values of the parameter w_a has been illustrated in Fig. 2.5. It is seen that the field emission current (J_{fe}) strongly depends on the applied field and significantly contributes to the total current for large fields. The thermionic current (J_{th}) also increases monotonically with increasing f , with a slower rate than J_{fe} . The dependence of these currents on parameter w_a can easily be understood in terms of transmission coefficient dependence on potential energy barrier height. It may be noticed that the total emission current ($J_t = J_{th} + J_{fe}$) gets enhanced by a factor of about eight for $f = 2$ from its initial value (for $f = 0$).

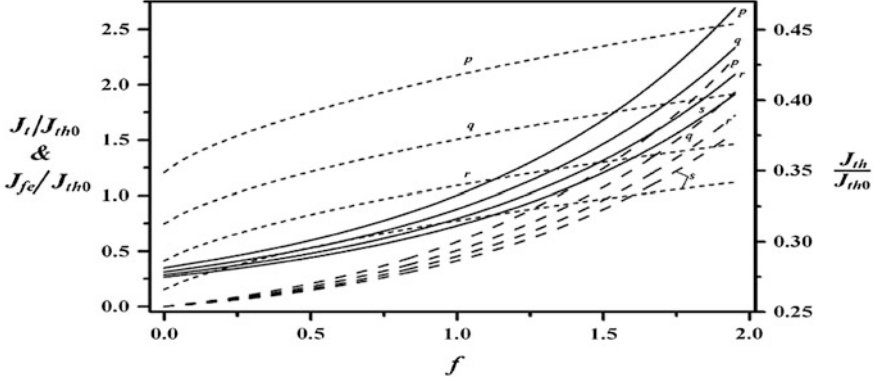


Fig. 2.5 Dependence of (J_{th}/J_{th0}) , (J_{fc}/J_{th0}) and (J_t/J_{th0}) with dimensionless electric field (f) for the parameters $T = 1000$ K and $v_0 = 1.0 \times 10^4$. The labels on the curves p , q , r and s correspond to $w_a = 60, 80, 100$ and 120 respectively. Dashed (left hand scale), short dashed (right hand scale) and solid curves (right hand scale) correspond to the field (J_{fc}/J_{th0}), thermionic (J_{th}/J_{th0}) and total (J_t/J_{th0}) emission current density respectively (after Agarwal et al. [1]; courtesy authors and publishers NRC Press)

2.2.3.4 Positively Charged Surface ($V_0 < 0$)

An electron can be emitted from a surface, charged to positive electric potential $(-V_0/e)$ only when its normal energy exceeds $W_a - V_0$.

Hence the thermionic emission current J_{th} and the mean energy of the emitted electrons far away from the surface is in the approximation $D(\epsilon_x) = 1$ given by

$$\begin{aligned} J_{th} &= -A_0 T^2 \exp[-(\varphi - v_0)] = -A_0 T^2 \exp[-(\Phi - V_0)/k_B T] \\ &= J_{th0} \exp(V_0/k_B T) \end{aligned} \quad (2.35c)$$

and

$$(\epsilon_{th})_{\text{far away}} = 2 \quad (2.36c)$$

In contrast to (2.36b), ϵ_{th} does not depend on v_0 . This is because the net effect of the positive potential is to enhance the work function and ϵ_{th0} is independent of the work function. In fact in the evaluation of J_{th} and ϵ_{th} only electrons with energy in excess of $W_a - V_0$ are considered.

2.2.4 Photoelectric and Light Induced Field Emission from a Plane Surface

A quantitative theory for the rate of photoelectric emission from a plane metallic surface was first formulated by *Fowler* [13, 14] on the basis of the following explicit and implicit assumptions:

- I. The free electron theory is applicable.
- II. Free electrons incident on a unit area of the surface (from inside) have a probability of absorbing a photon, which is proportional to the number of incident photons per unit area per unit time (the absorption occurs on the surface of the metal and does not alter the number of incident electrons on the surface from inside).
- III. The normal energy of an electron (due to the velocity component, normal to the surface) gets enhanced by $h\nu$ after absorption of a photon of frequency ν at the surface, where h is Planck's constant.
- IV. Electrons with a normal energy, exceeding the potential energy barrier at the surface get emitted.

A little later than Fowler [13], DuBridge [11] presented a similar theory for photoelectric emission; however instead of assumptions (ii) and (iii) DuBridge [11] assumed that

- (iia) The absorption of a photon by the electron occurs inside the metal and the number of such absorptions per unit volume is proportional to the number density of free electrons; the implicit assumption that this number is also proportional to the number of incident photons per unit area per unit time was not mentioned by him. Since he did not consider collisions of the electrons after absorption of photon, it is implied that the absorption was assumed to occur close to the surface, within a thickness much less than the mean free path of the electrons and
- (iiia) The total (not the normal) energy of an electron gets enhanced by $h\nu$ after the absorption of the photon.

In his derivation of the energy distribution of emitted photoelectrons and the emitted photoelectric current, DuBridge [11] made two further simplifications without justification viz.

- (i) The energy of the electron after absorption of a photon is much larger than $h\nu$ (footnote on p. 735 of his paper) and
- (ii) The normal energy of electrons after absorption of photons is just equal to the potential energy barrier at the surface [paragraph after (25) of his paper].

Usually the environment in which the photoelectric emission is of interest is at a temperature of 300 K, which corresponds to a thermal energy of electrons of the order of 0.04 eV, which is negligible as compared to the work function of the metal (which is the minimum value of $h\nu$ of interest). Hence in general the ratio of

Table 2.3 Characteristics of four models of photoelectric emission

S.No.	Model	Absorption of photon	Enhancement of energy
Ia.	Fowler [13] plus transmission coefficient	Surface	Normal
Ila.	Modified <i>DuBridge</i> [11] (without simplifications)	Inside	Total
Ib.	A	Inside	Normal
Ilb.	B	Surface	Total

the energy of the electron after absorption of the photon to $h\nu$ is of the order of unity and certainly not much larger than one, as assumed by DuBridge [11]. The second assumption implies the neglect of electrons of normal energy, significantly higher than that corresponding to the potential energy barrier at the surface. This also severely limits the applicability of the theory.

Fowler [13] has analyzed the effect of the dependence of the boundary transmission coefficient and the probability of absorption of a photon by an electron on the energy of the emitted electrons. It was seen that the observed dependence of the photoemission current on the temperature and frequency was in slightly better agreement with experiments, when these parameters were assumed to be independent of the electron energy than the case when the energy dependence was taken into account. A critique of the later work which justifies the adequacy of the assumptions of Fowler [13] and DuBridge [11] has been given by Dewdney [9].

In view of the arbitrariness of the assumptions, made by Fowler [13] and DuBridge [11] it is desirable, to also investigate the problem, based on the following alternate (but equally arbitrary) assumptions:

- A. Electrons absorb a photon inside the metal and the normal (not total) energy gets enhanced by $h\nu$.
- B. Electrons absorb a photon at the surface and the total energy (not normal energy) gets enhanced by $h\nu$.

The characteristics of four models for photoelectric emission are outlined in Table 2.3.

Detailed computations highlight the fact that the important aspect is the mode of absorption of the photons by the free electrons (enhancement of normal or total energy) and not the site of absorption viz. inside the metal or on the surface. Hence, only cases Ia and Ila viz. *Fowler's* and *Dubridge's* models have been considered in this chapter.

A number of papers have been published on different aspects of photoelectric emission. Most of these are concerned with basic derivation of $\beta(E, \nu)$, the probability of absorption of a photon by an electron of energy E , based on different models and mathematical techniques. Some are concerned with surface states, multiphoton absorption, discussion of specific emitters and the band structure of the material, Auger process and elastic as well as inelastic collisions of electrons, within the emitting material. These theories are material-specific and do not have

the general applicability of the models in Table 2.3. Moreover, Fowler [13] presented results in a user friendly mode; these have been used frequently by the investigators. Most of these investigations assumed that the probability of emission of an electron having a normal energy greater than the surface potential energy barrier is unity; this assumption is valid from classical considerations but is untenable in wave mechanics.

2.3 Fowler's Theory (Case: Ia) (After Fowler et al. [13])

2.3.1 Uncharged Surface

In view of *Fowler's* assumption (ii), the electrons, hitting the surface per unit time per unit area d^2n_1 have a probability $\beta(v)A(v)$ of absorbing a photon of frequency v , where $A(v)$ is the number of incident photons per unit area per unit time and $\beta(v)$ is indicative of the efficiency of the absorption of photons by electrons, incident on the surface; the energy of the absorbed photon enhances the normal energy of the electrons. Hence, using (2.9) the number of photoelectrons (electrons, which have absorbed a photon), hitting the surface per unit area per unit time is

$$d^2n_{ph} = (A_0/e)T^2\beta(v)A(v)F_D(\varepsilon_x + \varepsilon_t - \varepsilon_F)d\varepsilon_x d\varepsilon_t.$$

Putting $\varepsilon'_x = \varepsilon_x + \varepsilon_v$ (where $\varepsilon_v = hv/k_B T$ where ε'_x is the normal energy of an electron with energy ε_x after absorption of a photon) in the above equation one obtains

$$\begin{aligned} d^2n_{ph} &= (A_0/e)T^2\beta(v)A(v)F_D(\varepsilon'_x + \varepsilon_t - \varepsilon_v - \varepsilon_F)d\varepsilon'_x d\varepsilon_t. \\ &= (A_0/e)T^2\beta(v)A(v)F_D(\varepsilon''_x + \varepsilon_t + w_a - \varepsilon_v - \varepsilon_F)d\varepsilon''_x d\varepsilon_t, \end{aligned} \quad (2.39)$$

where $\varepsilon''_x = \varepsilon'_x - w_a$ is the energy of a photoelectron after crossing the surface energy barrier w_a .

Integrating d^2n_{ph} over $0 < \varepsilon_t < \infty$ one obtains

$$dn_{ph} = (A_0/e)T^2\beta(v)A(v)\ln[1 + \exp(\varepsilon_v + \varepsilon_F - \varepsilon'_x)]d\varepsilon'_x. \quad (2.40)$$

Hence the number of photoelectrons emitted due to the photoelectric effect is given by

$$\begin{aligned} n_{ph} &= (-J_{ph}/e) = (A_0/e)T^2\beta(v)A(v) \int_{w_a}^{\infty} D(\varepsilon'_x) \ln[1 + \exp(\varepsilon_v + \varepsilon_F - \varepsilon'_x)]d\varepsilon'_x, \\ &= (A_0/e)T^2\beta(v)A(v) \int_0^{\infty} D(\varepsilon''_x + w_a) \ln[1 + \exp(\zeta - \varepsilon''_x)]d\varepsilon''_x, \end{aligned} \quad (2.41a)$$

where $\varepsilon_x'' = \varepsilon_x' - w_a$ is the energy of a photoelectron after emission,

$$\xi = \varepsilon_v - [w_a - \varepsilon_F] = \varepsilon_v - \varphi = (h\nu - \Phi)/k_B T$$

and $\Phi = W_a - E_F$ is the work function of the material.

Putting $D(\varepsilon_x'' + w_a) = 1$ as is usually the practice and $\exp(\xi - \varepsilon_x'') = \zeta$ one obtains the current density due to photoelectron emission

$$J_{ph} = -en_{ph} = -A_0 T^2 \beta(\nu) A(\nu) \Phi_0(\xi), \quad (2.41b)$$

where

$$\Phi_0(\xi) = \int_0^{\exp \xi} \frac{\ln[1 + \zeta]}{\zeta} d\zeta. \quad (2.41c)$$

As discussed earlier, in general $D(\varepsilon_x')$ is not unity but given by (2.17) for an electrically neutral surface.

However in case $D(\varepsilon_x'' + w_a) = 1$, as is usually assumed the mean energy of the emitted photoelectrons, just outside the surface is

$$\begin{aligned} \langle \varepsilon'' \rangle &= \frac{\int_0^\infty \int_0^\infty (\varepsilon_x'' + \varepsilon_t) d^2 n_{ph}}{\int_0^\infty \int_0^\infty d^2 n_{ph}} \\ &= \frac{\int_0^\infty \int_0^\infty (\varepsilon_x'' + \varepsilon_t) F_D(\varepsilon_x'' + \varepsilon_t - \xi) d\varepsilon_x'' d\varepsilon_t}{\int_0^\infty \int_0^\infty F_D(\varepsilon_x'' + \varepsilon_t - \xi) d\varepsilon_x'' d\varepsilon_t}. \end{aligned}$$

Using identity (2.37) the above equation reduces to

$$\begin{aligned} \langle \varepsilon'' \rangle &= \frac{\int_0^\infty \varepsilon''^2 F_D(\varepsilon'' - \xi) d\varepsilon''}{\int_0^\infty \varepsilon'' F_D(\varepsilon'' - \xi) d\varepsilon''} \\ &= \frac{1}{\Phi_0(\xi)} \int_0^\infty 2\varepsilon'' \ln[1 + \exp(\xi - \varepsilon'')] d\varepsilon''. \end{aligned} \quad (2.42a)$$

It is useful to define photoelectric efficiency $\chi(\nu)$ as the number of photoelectrons emitted per incident photon. Thus

$$\chi(\nu) = n_{ph}/A(\nu).$$

The best fit of experimental data for dependence of $\chi(\nu)$ on ν is as follows

$\chi(\nu)/\chi_m = (729/16)(\nu_0/\nu)^4(1 - \nu_0/\nu)^2$ (Spitzer [64]; Sodha et al. [49] and $\chi(\nu)/\chi_m = (1 - \nu_0/\nu)^2$ [7] where ν_0 is threshold frequency and χ_m is the maximum value of χ .

It is seen that for $\xi > 5$, $\langle \varepsilon'' \rangle \approx 0.472 + 0.657\xi$ to an excellent approximation.

2.3.1.1 Negatively Charged Surface ($v_0 > 0$)

Equations (2.41a), (2.41b) and (2.42a, 2.42b) for the current density and mean energy of electrons are valid for a negatively charged surface when w_a is replaced by $w_a - \alpha f^{1/2}$ and appropriate data for $D(\epsilon'_x)$ is used. Further the mean energy away from the surface is $\epsilon''_{\text{faraway}} = \langle \epsilon'' \rangle + v_0$.

2.3.2 Positively Charged Surface ($v_0 < 0$)

As in the case of thermionic emission the expressions for J_{ph} and $\langle \epsilon'' \rangle$ (far away from the surface) is obtained by putting $w_a - v_0$ for w_a . Thus

$$J_{\text{ph}} = J_{\text{ph}} = -en_{\text{ph}} = -A_0 T^2 \beta(v) A(v) \Phi_0(\xi + v_0) \quad (2.41d)$$

and

$$\langle \epsilon'' \rangle_{\text{far away}} = \frac{1}{\Phi_0(\xi + v_0)} \int_0^\infty 2\epsilon'' \ln[1 + \exp(\xi + v_0 - \epsilon'')] d\epsilon'' \quad (2.42b)$$

2.3.3 Light Induced Field Emission

For a negatively charged surface, the current density J_{fp} (in analogy with (2.41a)) on account of tunneling of low energy photoelectrons ($\epsilon'_x < w_a - \alpha f^{1/2}$) is given by

$$J_{\text{fp}} = -en_{\text{life}} = -A_0 T^2 \beta(v) A(v) \int_0^{w_a - \alpha f^{1/2}} D(\epsilon'_x) \ln[1 + \exp(\epsilon_v + \epsilon_F - \epsilon'_x)] d\epsilon'_x$$

for $v_0 > w_a$

(2.43a)

and

$$J_{\text{fp}} = -en_{\text{life}} = -A_0^2 T^2 \beta(v) A(v) \int_{w_a - \alpha f^{1/2} - v_0}^{w_a - \alpha f^{1/2}} D(\epsilon'_x) \ln[1 + \exp(\epsilon_v + \epsilon_F - \epsilon'_x)] d\epsilon'_x$$

for $v_0 < w_a$

(2.43b)

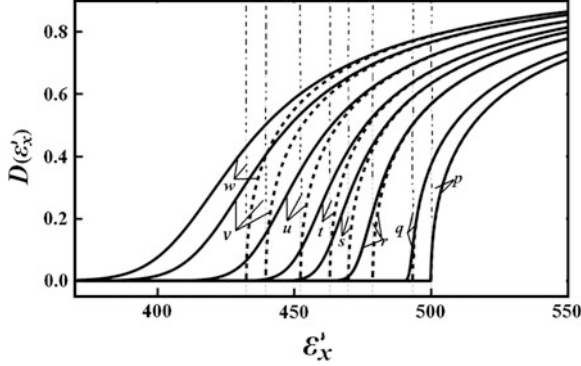


Fig. 2.6 Dependence of $D(\varepsilon'_x)$ on ε'_x for the parameters $T = 300$ K, $w_a = 500$ and $v_0 = 1.0 \times 10^4$. The labels on the curves p, q, r, s, t, u, v and w correspond to $f = 0, 1, 10, 20, 30, 50, 80$, and 100 , respectively. The *solid curves* correspond to the present analysis while *dashed curves* refer to the step potential barrier with reduced height. The portion of the curves corresponding to *left- and right-hand side of the vertical lines* refer to the light induced field emission (life) and photoelectric emission, respectively (after Agarwal et al. [1]; curtesy authors and publishers NRC Press)

This phenomenon was predicted by Sodha et al. [41] and verified experimentally by Kher et al. [23] and Iwami et al. [21]. The prediction of (2.43a), (2.43b) that J_{fp} is proportional to the light irradiation $\lambda(v)$ is in accordance with the observations of Iwami et al. [21]; other theories do not explain this observation.

2.3.4 Numerical Results and Discussions

Figures 2.6 and 2.7 illustrate the dependence of $D(\varepsilon'_x)$ on ε'_x for a temperature of 300 K; the variation is similar to that in Figs. 2.2 and 2.3, corresponding to a temperature of 1000 K.

The dependence of light-induced field emission (*life*) (J_{fp}/J_{ph0}) and photo-emission (J_{ph}/J_{ph0}) currents on the dimensionless field strength (f) for different values of the parameters ε_v and φ has been illustrated in Figs. 2.8 and 2.9. Figure 2.8 indicates that the photoemission current (J_{ph}/J_{ph0}) increases with increasing field strength and parameter ε_v ; this is because of large availability of high energy electrons and corresponding smaller energy barrier height. The *life* current (J_{fp}) displays a trend opposite to that in case of J_{ph} with increasing ε_v ; this is explained on the basis of large availability of low energy electrons for tunneling for small ε_x . The parameters J_{ph} and J_{fp} are indicative of the effect of the electric field f on the ε_x dependence of $D(\varepsilon_x)$. The effect of the work function of the metallic plate (φ) on emission currents has been displayed in Fig. 2.9. It is noticed that the current dependence (J_{ph} and J_{fp}) on φ displays a trend opposite to that in the case of ε_v ; this nature can be understood in terms of $\varsigma (= \varepsilon_v - \varphi)$, which

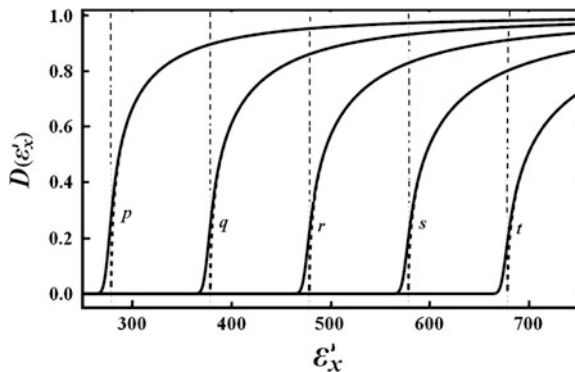


Fig. 2.7 Dependence of $D(\epsilon'_x)$ on ϵ'_x for the parameters $T = 300$ K, $f = 10$ and $v_0 = 1.0 \times 10^4$. Curves p , q , r , s and t correspond to $w_a = 300, 400, 500, 600$, and 700 , respectively. The nature of the curves (solid, dashed and vertical lines) is the same as in Fig. 2.6 (after Agarwal et al. [1]; curtsey authors and publishers NRC Press)

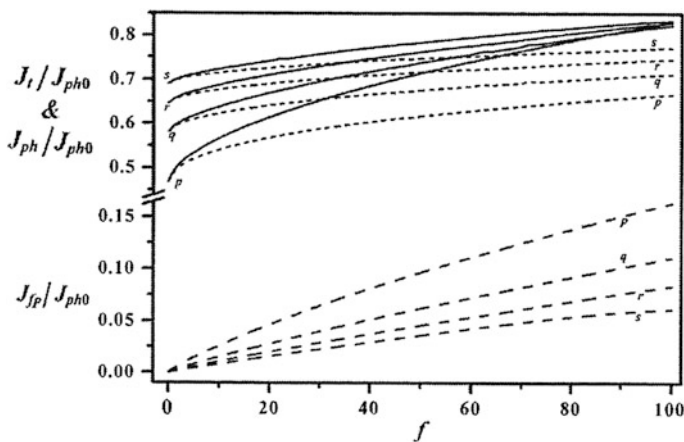


Fig. 2.8 Dependence of (J_{ph}/J_{ph0}) , (J_{ip}/J_{ph0}) and (J_t/J_{ph0}) on dimensionless electric field (f) for the parameters $T = 300$ K, $w_a = 500$ and 120 and $v_0 = 1.0 \times 10^4$. Dashed, short dashed and solid curves correspond to $\phi = 200$. The labels on the curves p , q , r and s correspond to $\epsilon_v = 250, 300, 350$, and 400 , respectively. Dashed (left-hand scale), short dashed (right-hand scale) and solid curves (right hand scale) correspond to the life (J_i/J_{ph0}), photo (J_{ph}/J_{ph0}) and total (J_t/J_{ph0}) emission current density, respectively (after Agarwal et al. [1]; curtsey authors and publishers NRC Press)

increases with increasing ϵ_v and decreasing ϕ . The figures also display the fact that *life* current significantly contributes to the total emission current ($J_t = J_{ph} + J_{ip}$) for large f ; it is also interesting to point out that the total current enhances by a factor of about 1.5 from its initial value (at $f = 0$) for the chosen set of parameters.

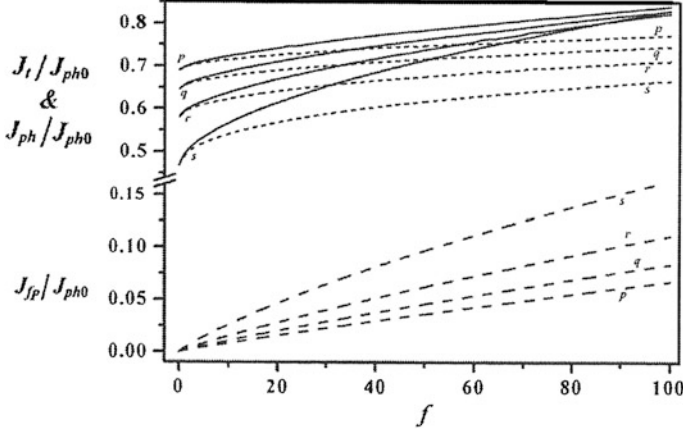


Fig. 2.9 Dependence of (J_{ph}/J_{ph0}) , (J_{fp}/J_{ph0}) and (J_t/J_{ph0}) on dimensionless electric field (f) for the parameters $T = 300\text{ K}$, $w_a = 500$ and 120 and $v_0 = 1.0 \times 10^4$. *Dashed, short dashed and solid curves* correspond to $\varepsilon_v = 300$. The labels on the curves p , q , r and s correspond to $\varphi = 100, 150, 200$ and 250 respectively. *Dashed (left hand scale), short dashed (right hand scale) and solid curves (right hand scale)* correspond to the life (J_{fp}/J_{ph0}), photo (J_{ph}/J_{ph0}) and total (J_t/J_{ph0}) emission current density respectively (after Agarwal et al. [1]; courtesy authors and publishers NRC Press)

2.4 Modified Dubridge Theory: Case IIa and other effects

According to this theory, the total (not normal) energy of an electron gets enhanced by $h\nu$ on absorption of a photon of frequency ν . Hence if p and p' denote the momentum of an electron before and after the absorption of a photon and E' is the energy of the electron after absorption of the photon [11].

$$E' = (p'^2/2m) = h\nu + (p^2/2m). \quad (2.44)$$

Hence from (2.8b) and (2.44) the momentum distribution of electrons after absorption of a photon is

$$n(p')dp' = (2/h^3)\beta(\nu)\Lambda(\nu)F_D(\varepsilon' - \varepsilon_v - \varepsilon_F)4\pi[1 - (\varepsilon_v/\varepsilon')]^{1/2}p'^2dp',$$

which is equivalent to

$$n(p')dp'_x dp'_y dp'_z = (2/h^3)\beta(\nu)\Lambda(\nu)F_D(\varepsilon' - \varepsilon_v - \varepsilon_F)[1 - (\varepsilon_v/\varepsilon')]^{1/2}dp'_x dp'_y dp'_z,$$

where $\varepsilon' = E'/k_B T$.

Out of the electrons having $\varepsilon' > w_a$, the fraction having $\varepsilon'_x > w_a$ is $[1 - (w_a/\varepsilon')]^{1/2}/2$.¹ Hence, the number of electrons emitted per unit area per unit time is

$$n_{\text{ph}} = \int_{\sqrt{2mW_a}}^{\infty} \int_{-\infty}^{\infty} \int_{-\infty}^{\infty} \bar{D}(\varepsilon'_x) [1 - (w_a/\varepsilon')]^{1/2} (p'_x/m) n(p') dp'_x dp'_y dp'_z.$$

As in the case of *Fowler's* theory, the above integral may be simplified as

$$\begin{aligned} n_{\text{ph}} &= (-J_{\text{ph}}/e) \\ &= (A_0/2e) T^2 \beta(v) A(v) \times \int_0^{\infty} \int_0^{\infty} D(\varepsilon''_x + w_a) \{1 - [w_a/(\varepsilon''_x + \varepsilon''_t + w_a)]^{1/2}\} \\ &\quad \{1 - [\varepsilon_v/(\varepsilon''_x + \varepsilon''_t + w_a)]\}^{1/2} F_D(\varepsilon''_x + \varepsilon''_t - \xi) d\varepsilon''_x d\varepsilon''_t, \end{aligned}$$

As an approximation $D(\varepsilon''_x + w_a)$ can be replaced by an average value $\bar{D}(\varepsilon'' + w_a)$,

$$\text{where } \varepsilon'' = \varepsilon''_x + \varepsilon''_t \text{ and } \bar{D}(\varepsilon'' + w_a) = \frac{1}{\varepsilon''} \int_0^{\varepsilon''} D(\varepsilon''_x + w_a) d\varepsilon''_x.$$

Thus using the identity $\int_0^{\infty} \int_0^{\infty} f(x_1 + x_2) dx_1 dx_2 = x \int_0^{\infty} xf(x)$

One obtains

$$\begin{aligned} n_{\text{ph}} &= (-J_{\text{ph}}/e) = (A_0/2e) T^2 \beta(v) A(v) \times \int_0^{\infty} \bar{D}(\varepsilon'' + w_a) \{1 - [w_a/(\varepsilon'' + w_a)]^{1/2}\} \\ &\quad \times \{1 - [\varepsilon_v/(\varepsilon'' + w_a)]\}^{1/2} \{1 + \exp(\varepsilon'' - \xi)\}^{-1} \varepsilon d\varepsilon \end{aligned} \quad (2.45)$$

The energy distribution of emitted photoelectrons, based on this theory is in a little better agreement with experiments than that corresponding to *Fowler's* theory. In view of the mathematically untreatable expressions occurring in *Dubridge's* theory, it has not been used to an appreciable extent in the study of the kinetics of complex plasmas. Hence, no further discussions of this theory has been made later in this book.

¹ The possible values of u_x, u_y, u_z corresponding to an electron speed u are the coordinates on the surface of a sphere of radius u . The area of the surface corresponding to $u_x > u_c$ is $2\pi(u - u_c)u$, while the area of the whole spherical surface is $4\pi u^2$. Hence the fraction of electrons with speed u having $u_x > u_c$ is simply

$$[2\pi u(u - u_c)/4\pi u^2] = 1/2(1 - u_c/u) = 1/2[1 - (w_a/\varepsilon')^{1/2}],$$

where $w_a = (m_e u_c^2/2)$ and $\varepsilon' = (m_e u^2/2)$.

2.5 Spicer's Three Step Model

No discussion of the photoelectric effect is complete, without a reference to the widely cited three step model, advanced by Spicer [52] and formalized by Bergland and Spicer [2]; a simple account of the model has been given by Spicer and Herrera-Gomez [53]. According to this model, photoemission of electrons is a bulk (rather than a surface) process and consists of three steps, viz

- (i) Generation of photoelectrons, (deep in material) having enough energy to overcome the surface barrier.
- (ii) Transport of these photoelectrons to the surface, taking into account the scattering of the electrons and
- (iii) Transmission through the surface.

Consider the normal incidence of light of frequency ν and irradiance $I_0(\nu)$ incident normally on the surface of a material with reflectivity $R(\nu)$. The irradiance $I(\nu)$ at the depth x in the material is given by

$$I(\nu) = I_0(\nu)[1 - R(\nu)] \exp[-\alpha(\nu)x], \quad (2.46)$$

where $\alpha(\nu)$ is the attenuation constant of light in the material and $R(\nu)$ is the reflection coefficient at the surface.

The number of photoelectrons with enough energy to escape from the surface, which is generated from photoexcitation per unit volume per unit time, is proportional to the irradiance. Hence, the number dn_{exc} of such photoelectrons generated per unit area in a thickness dx of the material is given by

$$dn_{\text{exc}} = \alpha_{\text{exc}} \cdot I \cdot dx, \quad (2.47)$$

where α_{exc} is a coefficient indicative of the efficiency of photoexcitation

The probability of traversing a distance x without significant loss of energy is given by

$$P_T(x) = \exp(-x/L). \quad (2.48)$$

where L is the mean free path of the electrons.

Hence, the number of photoelectrons emitted per unit area per unit time from the surface is

$$n_{\text{ph}} = \int_0^{\infty} P_{\text{em}}^{(\nu)} P_T(x) dn_{\text{exc}},$$

where $P_{\text{em}}^{(\nu)}$ is the probability of transmission through the surface barrier.

Substituting for $I(\nu)$, dn_{exc} and $P_T(x)$ from (2.46), (2.47) and (2.48) in the above equation and integrating the R.H.S. one obtains

$$n_{\text{ph}} = I_0(\nu)[1 - R(\nu)]\alpha\alpha_{\text{exc}}\{\alpha_{\text{exc}} + 1/L\}^{-1}. \quad (2.49)$$

The predictions for *Spicer's* model agree with experiments; however the inputs viz. absorption of the radiation in the solid, electron scattering/transport data and band structure are not available for many photoelectric surfaces. Further the computation, necessary for the application of *Spicer's* model is formidable. Hence phenomenological models, in good agreement with experiments are still relevant. In fact *Fowler's* expression for the photoelectric emission is still in vogue for interpretation of photoelectric data and models for physical processes, where photoelectric emission is important.

2.6 Size Effect

Watson [57, 58] adopted a simple model and predicted that the photoelectric efficiency χ of the surface of a particle of radius a is given by

$$(\chi/\chi_b) = \left(\frac{\beta_w}{\alpha_w}\right)^2 \frac{\alpha_w^2 - 2\alpha_w + 2 - 2\exp(-2\alpha_w)}{\beta_w^2 - 2\beta_w + 2 - 2\exp(-2\beta_w)} \quad (2.50)$$

where $\alpha_w = \alpha\alpha + a/L$, $\beta_w = \alpha\alpha$.

2.7 Secondary Electron Emission

2.7.1 Secondary Electron Emission by Electron Impact

When a high energy primary electron is incident on the surface of a material, it may either be reflected or enter the material. Once it is in the material, it may collide with scattering centers and ultimately get out of the material; this process is known as back scattering. However, some of the energy of the electron may be utilized in the excitation of electrons, which may escape from the material; this process is known as secondary electron emission.

The reflection coefficient is of the order of 0.05 at low energies of primary electrons and it rapidly decreases with increasing energy of primary electrons [19]. Both reflection and back scattering are not of importance in the kinetics of complex plasmas and therefore not considered hereinafter.

In what follows a phenomenological theory of secondary electron emission from (i) plane surface of a semi infinite solid and (ii) spherical grain has been presented. The case of a cylindrical surface has been discussed in Appendix B of this chapter.

2.7.1.1 Plane Surface of Semi-infinite Solid (After Jonker [20])

Jonker [20] has given a theory of secondary electron emission from the plane surface of a semi-infinite solid on account of the incidence of primary high energy electrons. The following four assumptions made by him constitute the basis of his theory as well as subsequent theories, including this presentation: (i) The primary electrons loose energy according to Whiddington's [59] law and that the absorption and scattering of electrons is negligible, (ii) The number of secondary electrons generated by a primary electron is proportional to the rate of energy loss in the solid, (iii) The absorption of secondary electrons in the material follows the exponential law and (iv) The distribution of generated secondary electrons is isotropic. Further for the sake of simplicity, it has also been implicitly assumed that V_p , the energy of the incident electron is much larger than the surface energy barrier.

The energy $V(x)$ in eV of a primary electron in a solid is given by [59]

$$V^2(x) = V_p^2 - \alpha x \quad (2.51)$$

where

V_p is the electron energy at $x = 0$,
 x is the distance traversed in cm and
 α is a constant dependent on the material.

The rate of secondary electron production n_s is proportional to the energy loss per unit length; thus the rate of secondary electron production in a distance dx is as per Bruining [3]

$$n_s dx = -KI_p \frac{dV(x)}{dx} dx = (K\alpha I_p/2)(V_p^2 - \alpha x)^{-1/2} dx, \quad (2.52)$$

where I_p is the primary beam current, i.e., number of primary electrons, incident on the surface per unit time and K is a material specific constant.

Consider the normal (along x direction) incidence of a beam of primary (high energy) electrons on the plane surface ($x = 0$) of a semi-infinite solid substance. The secondary electrons, generated at x (the distance from the surface) and moving in a direction making an angle between θ and $\theta + d\theta$ with the axis (corresponding to a solid angle $2\pi \sin\theta d\theta$), traverse a distance $x \sec\theta$, before hitting the surface and getting emitted. Hence the number of such secondary electrons getting emitted from the surface is from 2.51 and 2.52 given by

$$di_s = (K\alpha I_p/2)(V_p^2 - \alpha x)^{-1/2} dx \int_0^{\pi/2} \frac{2\pi \sin\theta d\theta}{4\pi} \exp(-\beta x \sec\theta) d\theta, \quad (2.53)$$

where β is the attenuation constant for secondary electrons and $(2\pi\sin\theta d\theta/4\pi)$ is the fraction of electrons emitted, making an angle between θ and $\theta + d\theta$ with the normal.

Integrating the above equation in the limit $x = 0$ to $x = x_m = V_p^2/\alpha$ (corresponding to $V(x) = 0$) one obtains.

$$I_s = (K\alpha I_p/4) \int_0^{x_{\max}} (V_p^2 - \alpha x)^{-1/2} dx \int_0^{\pi/2} \exp(-\beta x \sec\theta) \sin\theta d\theta. \quad (2.54a)$$

where $x_m = V_p^2/\alpha$ is the depth of penetration of the primary electron in the material and corresponds to $V(x_m) = 0$.

It is common to express the results in terms of secondary yield $\delta(V_p)$, defined as

$$\delta(V_p) = I_s/I_p. \quad (2.54b)$$

In case of oblique incidence at an angle λ to the normal, the distance of the point x from the surface is $x\cos\lambda$ and hence

$$I_s = (K\alpha I_p/4) \int_0^{x_{\max}} (V_p^2 - \alpha x)^{-1/2} dx \int_0^{\pi/2} \exp(-\beta' x) \sin\theta d\theta, \quad (2.54c)$$

where $\beta' = \beta\cos\lambda$.

If $I'_p(V_p)dV_p$ is the energy distribution of the primary beam the secondary current i_s is

$$i_s = \int \delta(V_p) I'_p(V_p) dV_p \quad (2.54d)$$

The various approaches to the evaluation of secondary electron emission essentially differ in the expressions for the rate of energy loss by primary electrons. A popular empirical expression for $\delta(V_p)$, number of secondary electrons emitted by the incidence of primary electrons of energy V_p is Sternglass [55], Jonker [20], Meyer-Vernet [26] is

$$\delta(V_p) = 7.4\delta_m(V_p/V_m) \exp[-2(V_p/V_m)^{1/2}], \quad (2.55)$$

where the maximum value of $\delta = \delta_m$ occurs for $V_p = V_m$.

Representative values [60] of δ_m and V_m are given in Table 2.4.

The energy distribution of secondary electrons is approximately Maxwellian with a characteristic energy of 2 eV (Hachenberg and Brauer [18]).

The electron emission on account of electron beams has been discussed in literature.

Table 2.4 Values of δ_m and V_m

Material	SiO ₂	MgO	Teflon	Kapton	Al ₂ O ₃	Mg	Al
δ_m	2.4	4.0	3.0	2.1	1.5–1.9	0.92	0.97
V_m (keV)	0.4	0.4	0.3	0.15	0.35–1.3	0.25	0.3

2.7.2 Spherical Particle (After Misra et al. [31])

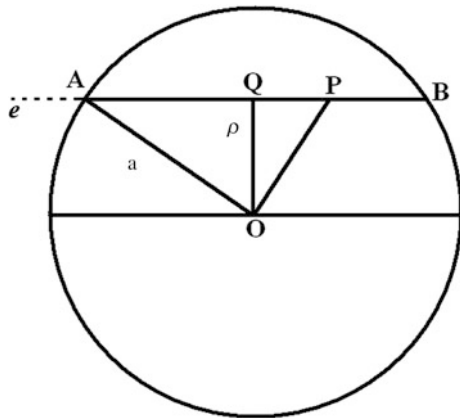
On the basis of rather simple analysis Draine and Salpeter [65] have emphasized the importance of secondary electron emission in the charging of small grains (≈ 10 nm or less in radius) when the penetration depth x_m of the primary electrons exceeds the diameter of the grains. In view of the existence of such small particles in the interstellar medium (Puget and Leger [66]) and space, e.g., *Hailey's* comet environment (Sagdeev et al. [67]), this phenomenon is of much interest in the charging of dust. A theory of the secondary electron emission and charging of a dust particle, exposed to high energy electrons (from the plasma or elsewhere) should also be of interest to situations other than those in space environment.

Meyer-Vernet [26] developed an elaborate theory for the charging of a dust particle in space, taking into account the phenomenon of secondary electron emission; however this theory was based on the widely used empirical relation by Sternglass [55]. However the validity of the results is severely limited by the fact that this relation is applicable only for the plane surface of the semi-infinite solid and hence completely ignores the effect of the size and shape of the particle.

Chow et al. [5] modified the theory by Jonker [20] to make it applicable to spherical particles and applied it to investigate the charging of the particles in *Maxwellian* and *Lorentzian* plasmas. The theory distinguishes between the cases when the diameter of the particle is larger or smaller than the penetration depth of the electrons. However the relevance of the theory is limited because it overlooks the following points: (i) The length of an electron path (AB) in the spherical particle depends on the perpendicular distance (ρ) from the center of the particle; hence it varies from *zero* to the diameter or x_m depending upon ρ (see Fig. 2.10), (ii) As a corollary to (i), when the diameter exceeds the penetration depth x_m there is an optimum perpendicular distance ρ_m from the center (corresponding to the path length equal to the penetration depth x_m) such that electrons corresponding to $\rho \geq \rho_m$ will pass through the particle while the electrons, corresponding to $\rho < \rho_m$ will get stuck in the particle and (iii) The electrons, stuck in the particle and primary electrons sticking to the surface contribute to the charging of the particles.

Here we have modified the theory of Chow et al by incorporating the points, enumerated above. Specifically the parameter δ (the number of secondary electrons, emitted by the particle per primary electron) has been evaluated as a function of primary electron energy, radius, and electric potential of the particle. The parameter δ for *Maxwellian distribution* of the primary electron energy has also been evaluated.

Fig. 2.10 Path of incident primary electron in a particle



Referring to Fig. 2.10, considering the four basic assumptions [20] stated earlier and using (2.52), the rate of secondary electron generation induced by a primary electron in traversing a distance dx in the substance is given by [5]

$$\begin{aligned} dn_s &= (K\alpha/2)(V_p^2 - \alpha x)^{-1/2} \langle \exp[-\beta l(x, \rho, \theta, \varphi)] \rangle dx \\ &= (K\alpha/2)(V_p^2 - \alpha x)^{-1/2} f(x, \rho) dx, \end{aligned} \quad (2.56)$$

where K is a constant for a given material, β is the attenuation constant for the secondary electrons in the substance, l is the distance of any point (θ, φ) on the spherical surface ($r = a$) from P and $\langle \rangle$ denotes the average over all points on the sphere. To determine the distance l of point P from any point on the sphere viz. $(a \cos \theta \cos \varphi, a \cos \theta \sin \varphi, a \sin \theta)$, one may without loss of generality consider $z = 0$, to be the plane containing the center of particle and the path. Thus one has

$$l^2(x, \theta, \varphi, \rho) = \left[[a \cos \theta \cos \varphi - [x - (a^2 - \rho^2)^{1/2}]]^2 + (a \cos \theta \sin \varphi - \rho)^2 + a^2 \sin^2 \theta \right].$$

Hence

$$f(x, \rho) = \langle \exp(-\beta l) \rangle = \frac{1}{4\pi} \int_{\theta=0}^{\pi} \int_{\varphi=0}^{2\pi} \exp[-\beta l(x, \theta)] \sin \theta \, d\theta \, d\varphi. \quad (2.57)$$

It is convenient to define a value of $\rho = \rho_m$ so that the path length of the electron in the particle is x_m , the penetration depth; thus $\rho_m^2 = a^2 - (x_m/2)^2$. It may be noted that for $x_m < 2a$, when $\rho < \rho_m$, $AB > x_m$ and the primary electron gets stuck in the particle; when $\rho > \rho_m$, $AB < x_m$ and the electron passes through the particle. In case $x_m > 2a$, all the electrons pass through the particle.

Consider a mono-energetic beam of primary electrons with n_e electrons incident per unit area, per unit time, normal to the direction of the beam. The number of

primary electrons incident per unit cross section of the dust surface normal to the beam, per unit time n_p is given by (Abbas et al. [68])

$$n_p = n_e[1 - (V_s/V_p)] \quad (2.58)$$

where V_s is the potential energy of the electron at the surface of the particle and $V_s \ll V_p$.

Hence, the number of secondary electrons produced per unit time is

$$n_s = (1 - \eta_s) \left(\frac{K\alpha}{2} \right) \left[\int_0^{\rho_m} 2\pi n_p I_1(V_p, \rho) \rho d\rho + \int_{\rho_m}^a 2\pi n_p I_2(V_p, \rho) \rho d\rho \right] \quad \text{for } x_m < 2a \quad (2.59a)$$

and

$$n_s = (1 - \eta_s) \left(\frac{K\alpha}{2} \right) \int_0^a 2\pi n_p I_2(V_p, \rho) \rho d\rho \quad \text{for } x_m \geq 2a \quad (2.59b)$$

where

$$I_1(V_p, \rho) = \left(\int_0^{x_m} (V_p^2 - \alpha x)^{-1/2} f(x, \rho) dx \right),$$

$$I_2(V_p, \rho) = \left(\int_0^{2\sqrt{a^2 - \rho^2}} (V_p^2 - \alpha x)^{-1/2} f(x, \rho) dx \right)$$

and η_s is the electron sticking (at the surface) coefficient.

The secondary electron emission yield δ can be expressed as: $\delta = (n_s/\pi a^2 n_p)$.

In the dimensionless form δ viz. $\delta' = \delta/(1 - \eta_s)K\sqrt{a\alpha}$ can be expressed as a function of $\beta' = \beta a$, and $x'_m = (x_m/a)$; to do so one has to use $\mathbf{r} = a\mathbf{r}'$

For a charged particle, the yield $\delta(V_s)$ is given by⁶

$$\delta'(V_s) = \delta'(V_s = 0) \quad \text{for } V_s \geq 0 \quad (2.60a)$$

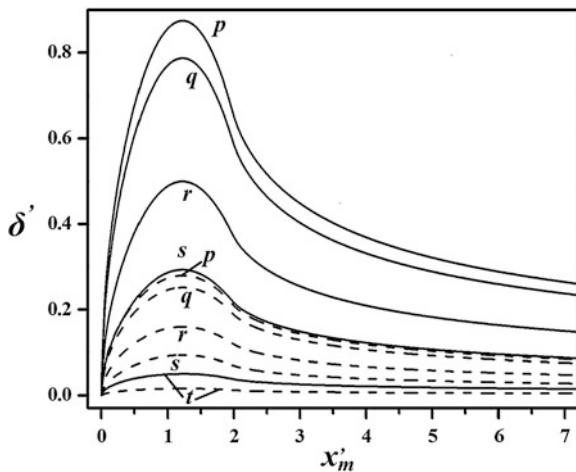
$$\delta'(V_s) = \kappa \delta'(V_s = 0) \quad \text{for } V_s < 0 \quad (2.60b)$$

where $\kappa = (1 - V_s/kT_s) \exp(V_s/k_B T_s)$ and T_s is the temperature of secondary electrons.

The dependence of δ' on x'_m has been illustrated for different values of β' in Fig. 2.11. It is seen that the yield (δ'_m) takes a maximum value for an optimum value of x'_m and it decreases with increasing β' (i.e., particle size).

When diameter of the particle exceeds the penetration distance, the number of primary electrons which gets stuck in the dust particle is given by

Fig. 2.11 Dependence of δ' on x'_m ; the labels p, q, r, s and t refer to $\beta' = 0.01, 0.1, 0.5, 1.0$ and 3.0 respectively for $b = 5a$. Solid and broken curves correspond to uniform and Gaussian distribution of electrons in the beam (after Misra et al. [31], curtsey authors and publishers AIP)



$$n_{\text{stuck}} = (1 - \eta_s) \int_0^{\rho_m} 2\pi n_p \rho d\rho = (\pi \rho_m^2)(1 - \eta_s)n_p. \quad (2.60c)$$

For a Gaussian beam of primary electrons of width b , n_p is not constant and may be expressed as

$$n_p = n_{p0} \exp(-\rho^2/b^2). \quad (2.61a)$$

With this modification (2.59a) and (2.59b) are valid, while (2.60c) changes to

$$n_{\text{stuck}} = n_{p0} \pi b^2 (1 - \eta_s) [1 - \exp(-\rho_m^2/b^2)] \quad (2.61b)$$

The secondary electron emission yield may be obtained by substituting $\pi b^2 [1 - \exp(-a^2/b^2)]$ instead of πa^2 in (60). Figure 2.11 indicates that the Gaussian profile of primary electron beam significantly suppresses the maximum value of the yield (δ'_m).

2.7.3 Spherical Particle in Maxwellian Plasma

Consider a spherical particle immersed in a plasma with high energy (primary) electrons having a *Maxwellian distribution* of energy. Following the well-established *Orbital Motion Limited (OML) approach*, the net electron flux incident on the dust particle can be expressed as (Sodha and Guha [46])

$$J_p = n_e (k_B T_e / 2\pi m_e)^{1/2} (1 - V_s / k_B T_e) \quad \text{for } V_s < 0 \quad (2.62a)$$

and

$$J_p = n_e (k_B T_e / 2\pi m_e)^{1/2} \exp(-V_s / k_B T_e) \quad \text{for } V_s \geq 0 \quad (2.62b)$$

Following the approach similar to the earlier analyses [5, 26], the net electron flux associated with secondary electron emission is given by

$$J_s = n_e (2\pi / m_e^2) (2\pi k_B T_e / m_e)^{-3/2} \kappa \int_0^\infty \varsigma_s(V_p)(V_p - V_s) \exp[-V_p / k_B T_e] dV_p$$

for $V_s < 0$

(2.63a)

and

$$J_s = n_e (2\pi / m_e^2) (2\pi k_B T_e / m_e)^{-3/2} \int_{V_s}^\infty \varsigma_s(V_p)(V_p - V_s) \exp[-V_p / k_B T_e] dV_p, \quad (2.63b)$$

for $V_s \geq 0$,

where

$$\varsigma_s = (1 - \eta_s)(K\alpha/2) \left[\int_0^{\rho_m} 2\pi I_1(V_p, \rho) \rho d\rho + \int_{\rho_m}^a 2\pi I_2(V_p, \rho) \rho d\rho \right] \quad \text{for } x_m < 2a, \quad (2.64a)$$

$$\varsigma_s = (1 - \eta_s)(K\alpha/2) \int_0^a 2\pi I_2(V_p, \rho) \rho d\rho \quad \text{for } x_m \geq 2a, \quad (2.64b)$$

and

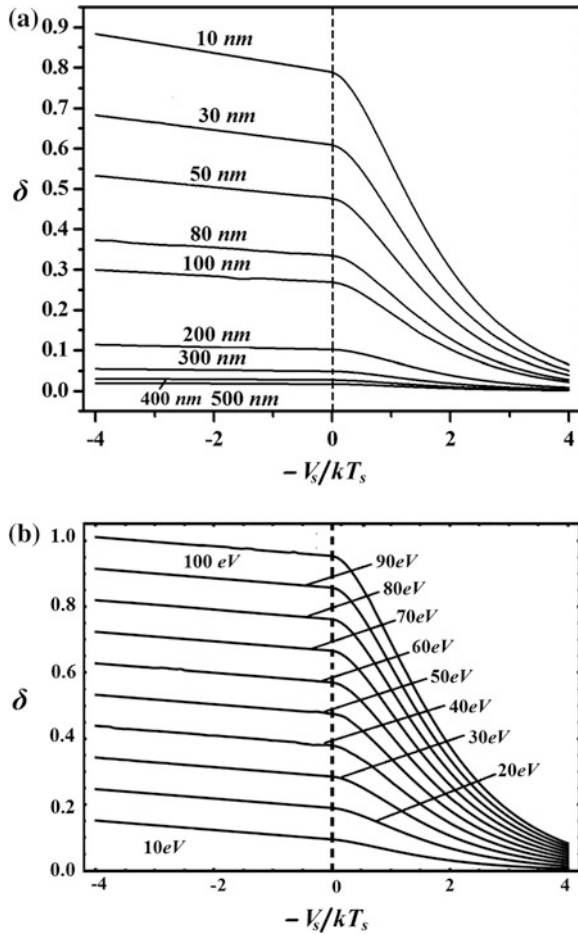
$$\kappa = 1 - (V_s / k_B T_e).$$

The secondary emission yield can be expressed as: $\delta = (J_s / J_p)$.

The effect of particle size and electron temperature on secondary emission yield (δ) for a particle in a Maxwellian plasma has been illustrated in Fig. 2.3a, b, for a standard set of parameters, viz. $a = 50$ nm, $k_B T_s = 3$ eV, $k_B T_e = 50$ eV, $\alpha = 10^{12}(\text{eV})^2/\text{cm}$, $\beta = 10^5/\text{cm}$, $K = 0.01/\text{eV}$ and $\mu_s = 0.1$. The figures indicate that δ linearly increases with increasing negative potential on the surface while it sharply decays with increasing positive potential. Increasing the size of the particle significantly reduces the generation of secondaries because of decreasing function $f(x, \rho)$, which leads to decrease in the secondary emission yield (δ); this nature has been displayed in Fig. 2.12. Further, the increase in the temperature of primary electrons ($k_B T_e$) enhances x_m and the accretion over dust surface, resulting in the increasing secondary yield (this behavior has been illustrated in Fig. 2.12).

(iii) Cylindrical Particles (see Appendix B).

Fig. 2.12 Dependence of δ on (V_s/kT_s) for different values of **a** radius (a, in nm) of the particle and **b** mean temperature (kT_e , in eV) of the incident primary electrons for standard set of parameters in the text; the magnitude of varying parameter (kT_e) has been indicated on the curves (after Misra et al. [31], courtesy authors and publishers AIP)



2.8 Electron Emission from Charged Spherical and Cylindrical Surfaces of Metals

2.8.1 What is Different About Electron Emission from Curved Surfaces?

Consider an electron just outside the surface (after overcoming the surface barrier) of a metal, charged to a potential $-(V_0/e)$.

The conditions for the electron to overcome the surface potential and thus get emitted are

- I. **Negatively Charged surface** (positive electron potential energy V_0 after emission of an electron): All such electrons will escape (or get emitted). Hence, the expressions for thermionic and photoelectric emission current and the mean energy, just outside the surface are identical to the case of uncharged plane surface.
- II. **Positively Charged surface** (negative electron potential energy $-V_0$ after emission of an electron just outside the surface):

1. *Plane surface:*

$$E_x (= m_e u_x^2 / 2) > V_0, \quad (2.65a)$$

2. *Spherical surface:*

$$E (= m_e u^2 / 2) > V_0, \quad (2.65b)$$

3. *Cylindrical surface:*

$$[E_x (= m_e u_x^2 / 2) + E_y (= m_e u_y^2 / 2)] > V_0, \quad (2.65c)$$

where \mathbf{u} is the velocity of the electron just outside the metal, \mathbf{x} is the direction, normal to a surface element and \mathbf{z} is the direction along the axis (in case 3 only).

Further since the expressions for the potential energy of an electron outside a metal, taking into account the image force are dependent on the nature of the surface, the reduction in the work function on account of a negative electric potential on the surface also depends on its nature. The expressions for the transmission coefficient also depend on the variation of electron potential energy with distance, which is determined by the shape of the surfaces.

2.8.2 Reduction of Work Function by Negative Electric Potential on a Spherical Surface

The potential energy $V(r)$ of an electron near the surface of a metallic spherical particle of radius a is given by [50]

$$V(r) = (-e^2/a)[2(r^2 - a^2) + e^2a/W_a]^{-1} + (e^2a/2r^2) + (Ze^2/r) \quad \text{for } r > a, \quad (2.66a)$$

and

$$V(r) = -[W_a - e^2/2a] + (Ze^2/a) \quad \text{for } r < a, \quad (2.66b)$$

where a is the radius of the particle, and $-Ze$ is the charge on the particle.

When e^2a/W_a is negligible as compared to $(r^2 - a^2)$ (2.66a) reduces to the usual expression, in text books (e.g., Page and Adams [33]).

Equation (2.66b) is the usual expression, except for a surface barrier $-[W_a - e^2/2a]$ instead of $-W_a$.

Based on (2.66a), Sodha and Sharma [50] tabulated the reduction in the work function $\Delta\phi/(e^2/a)$ as a function of the charge on the particle. An identical analysis was also made much later by [8]. Recently Sodha and Srivatsava [51] have made a similar analysis, taking into account the *Debye* shielding; thus (2.66a) gets replaced by

$$U(\rho) = -\{2(\rho^2 - 1) + (e^2/aW_a)\}^{-1} + (1/2\rho^2) + (Z/\rho) \exp[(1 - \rho)/\mu] \quad (2.66c)$$

for $\rho > 1$

and

$$U(\rho) = (Z + 1/2) - W_a/(e^2/a) \quad \text{for } \rho < 1, \quad (2.66d)$$

where $\rho = r/a$ and $U(\rho) = V(r)/(e^2/a)$.

The value of ρ corresponding to the maximum value of U viz. ρ_m can be obtained by putting by $(dU/d\rho) = 0$; thus

$$\mu\rho_m^4 - \mu(\rho_m^2 - 1)^2 + Z\rho_m(\rho_m^2 - 1)^2(\rho_m + \mu) \exp[(1 - \rho_m)/\mu] = 0.$$

It is seen that $(\rho_m^2 - 1)$ is in general much larger than e^2/aW_a .

Hence, the maximum value of the potential energy $U_m(Z, \mu)$ is given by

$$U_m(Z, \mu) = -[1/2(\rho_m^2 - 1)] + [1/2\rho_m^2] + (Z/\rho_m) \exp[(1 - \rho_m)/\mu] \quad (2.67)$$

In view of (2.66d), the energy E_F corresponding to *Fermi* level of a charged particle is given by

$$[E_F/(e^2/a)] = [E_{F0}/(e^2/a)] + (Z + 1/2) - [W_a/(e^2/a)],$$

where E_{F0} refers to an uncharged plane surface.

Hence the work function ϕ , corresponding to the charged particle is given by

$$\begin{aligned} [\phi/(e^2/a)] &= [(W_a - E_{F0})/(e^2/a)] + [U_m(Z, \mu) - (Z + 1/2)] \\ \text{or } (\phi - \phi_0)/(e^2/a) &= [\Delta\phi/(e^2/a)] = [U_m(Z, \mu) - (Z + 1/2)], \end{aligned} \quad (2.68)$$

where ϕ_0 refers to the work function of the uncharged plane surface and $\Delta\phi (= \phi - \phi_0)$ is the change in work function due to the charge and curvature of the surface of the particle.

Table 2.5 illustrates the dependence of $\Delta\phi/(e^2/a)$ on Z and μ . The *Coulomb limit* is approached when μ tends to infinity as given in Table 2.5.

Table 2.5 Dependence of $[-\Delta\phi/(e^2/a)]$ on Z and μ

$Z \rightarrow$	1	2	3	4	7	10	20	40	60	80	100	200	400
$\mu \downarrow$													
2	1.16	1.59	1.94	2.24	2.99	3.60	5.17	7.42	9.14	10.61	11.89	16.95	24.12
3	1.11	1.51	1.84	2.12	2.83	3.40	4.86	6.99	8.61	9.99	11.21	15.98	22.73
4	1.09	1.47	1.79	2.06	2.74	3.30	4.72	6.76	8.34	9.67	10.84	15.46	22.00
5	1.07	1.45	1.75	2.02	2.68	3.23	4.62	6.62	8.17	9.47	10.62	15.15	21.55
6	1.06	1.43	1.73	1.99	2.65	3.18	4.56	6.53	8.05	9.34	10.47	14.93	21.25
7	1.05	1.42	1.72	1.98	2.62	3.15	4.51	6.46	7.97	9.24	10.36	14.78	21.03
8	1.04	1.41	1.70	1.96	2.60	3.12	4.47	6.41	7.90	9.16	10.28	14.66	20.86
9	1.04	1.40	1.69	1.95	2.58	3.10	4.44	6.37	7.85	9.11	10.21	14.57	20.73
10	1.03	1.39	1.68	1.94	2.57	3.08	4.42	6.33	7.81	9.06	10.16	14.49	20.63
50	1.01	1.35	1.62	1.87	2.47	2.97	4.25	6.09	7.51	8.71	9.78	13.9	19.9
100	1.00	1.34	1.62	1.86	2.46	2.96	4.23	6.06	7.48	8.67	9.73	13.9	19.8
∞	1.00	1.34	1.61	1.85	2.45	2.94	4.20	6.03	7.44	8.63	9.68	13.8	19.7

After Sodha and Srivastava [23], curtesy authors and publishers Elsevier

2.8.3 Simple Theory of Electron Emission from Curved Surfaces

The theory presented in this section assumes that the transmission coefficient of an electron across the surface is unity when the normal energy is greater than W_a and is zero otherwise.

2.8.3.1 Negatively Charged Surfaces: ($V_s > 0$)

In the approximation, stated before, the rate and mean energy of emitted electrons (just outside the surface) are the same as in planar uncharged case. The mean energy far away from the surface gets enhanced by an amount equal to the potential energy of the electron at the surface. We have used the symbol V_0 for potential energy of an electron in case of a plane surface but it is convenient to use symbol V_s in case of curved surface.

2.8.3.2 Positively Charged Spherical Surfaces: ($V_s < 0$)

References [38, 39, 46] are relevant.

2.8.3.3 Thermionic Emission

The energy distribution of the number of electrons incident per unit area per unit time on the surface is given by

$$d^2n_1 = (A_0/e)T^2 \exp(-\varepsilon_x - \varepsilon_t + \varepsilon_F) d\varepsilon_x d\varepsilon_t. \quad (2.9)$$

The energy distribution just outside the surface (after the electrons have crossed the surface barrier $w_a (= W_a/k_B T)$) is

$$\begin{aligned} d^2n'_1 &= (A_0/e)T^2 \exp(-\varepsilon'_x - \varepsilon_t - w_a + \varepsilon_F) d\varepsilon'_x d\varepsilon_t \\ &= (A_0/e)T^2 \exp(-\varphi) \exp(-\varepsilon'_x - \varepsilon_t) d\varepsilon'_x d\varepsilon_t, \end{aligned} \quad (2.69)$$

where $\varepsilon'_x = \varepsilon_x - w_a$ denotes the normal energy of an electron just outside the surface and $\varphi = (w_a - \varepsilon_F) = (W_a - E_F)/k_B T$.

If the surface has an electrical potential $-V_s/e$ ($V_s < 0$), only electrons having a total energy larger than $-V_s$ or $(\varepsilon'_x + \varepsilon_t) > -v_s (= -V_s/k_B T)$ can escape from the surface and get emitted; in many publications instead of $-v_s$, $Ze^2/ak_B T = Z\alpha$ is used.

Hence from (2.69) the number of electrons n_{th} emitted from the surface per unit area per unit time is given by

$$\begin{aligned} (-J_{th}/e) &= n_{th} = (A_0/e)T^2 \exp(-\varphi) \int_0^\infty \int_0^\infty \exp(-\varepsilon'_x - \varepsilon_t) d\varepsilon'_x d\varepsilon_t \\ &\quad (\varepsilon'_x + \varepsilon_t) > -v_s \\ &= -(A_0/e)T^2 \exp(-\varphi) \int_{-v_s}^\infty \varepsilon \exp(-\varepsilon) d\varepsilon \\ &= -(A_0/e)T^2 (1 - v_s) \exp[-(\varphi - v_s)]; \end{aligned} \quad (2.70a)$$

In writing the single integral from the double integral identity (2.37) has been used.

In many investigations the term $(1 - v_s)$ is missing, which may be responsible for unacceptably large errors.

The mean energy of electrons, just outside the surface is from (2.69), given by

$$\begin{aligned} \varepsilon_{th0} &= [(A_0/e)T^2 \exp(-\varphi)/n_{th}] \cdot \int_0^\infty \int_0^\infty (\varepsilon'_x + \varepsilon_t) \exp(-\varepsilon'_x - \varepsilon_t) d\varepsilon'_x d\varepsilon_t \\ &\quad (\varepsilon'_x + \varepsilon_t) > -v_s \\ &= [\exp(-v_s)/(1 - v_s)] \int_{-v_s}^\infty \varepsilon^2 \exp(-\varepsilon) d\varepsilon \\ &= -v_s + (2 - v_s)/(1 - v_s) \end{aligned}$$

Hence, the mean energy far away from the surface is given by

$$\varepsilon_{\text{th}} = \varepsilon_{\text{th}0} + v_s = (2 - v_s)/(1 - v_s) \quad (2.70b)$$

For the evaluation of the integrals, occurring in the expressions for n_{th} and $\varepsilon_{\text{th}0}$ the identity from (2.37) has been used.

If we consider a particle of radius a with charge $(Z - 1)e$, it acquires a charge Ze after an electron gets outside the surface and hence the corresponding value of $-v_s$ is $Ze^2/ak_B T$.

2.8.3.4 Photoelectric Emission

From (2.39), the energy distribution of photoelectrons crossing the surface of the metal per unit area per unit time just outside the surface is given by.

$$d^2 n_{\text{ph}} = (A_0 T^2 / e) \beta(v) \Lambda(v) F_D(\varepsilon_x'' + \varepsilon_t - \zeta) d\varepsilon_x'' d\varepsilon_t, \quad (2.71)$$

where $\zeta = \varepsilon_v - [w_a - \varepsilon_F] = (h\nu - \Phi)/k_B T$.

Of these only those electrons can escape or be emitted for which $(\varepsilon_x'' + \varepsilon_t) > -v_s$. Hence

$$\begin{aligned} (-J_{\text{ph}}/e) = n_{\text{ph}} &= (A_0/e) T^2 \beta(v) \Lambda(v) \int_0^\infty \int_0^\infty F_D(\varepsilon_x'' + \varepsilon_t - \zeta) d\varepsilon_x'' d\varepsilon_t, \\ &\quad (\varepsilon_x'' + \varepsilon_t) > -v_s \\ &= (A_0/e) T^2 \beta(v) \Lambda(v) I_1(-v_s, \zeta) \end{aligned} \quad (2.72a)$$

and

$$\begin{aligned} \varepsilon_{\text{ph},0} &= [(A_0/e) T^2 \beta(v) \Lambda(v) / n_{\text{ph}}] \int_0^\infty \int_0^\infty (\varepsilon_x'' + \varepsilon_t - \zeta) F_D(\varepsilon_x'' + \varepsilon_t - \zeta) d\varepsilon_x'' d\varepsilon_t, \\ &\quad (\varepsilon_x'' + \varepsilon_t) > -v_s \\ &= (A_0/e) T^2 \beta(v) \Lambda(v) I_2(-v_s, \zeta) / n_{\text{ph}} \end{aligned} \quad (2.73a)$$

where using identity (2.37)

$$\begin{aligned}
I_1 &= \int_{-v_s}^{\infty} \varepsilon [1 + \exp(\varepsilon - \zeta)]^{-1} d\varepsilon \\
&= \{-\varepsilon \ln[1 + \exp(\zeta - \varepsilon)]\}_{-v_s}^{\infty} + \int_{-v_s}^{\infty} \ln[1 + \exp(\zeta - \varepsilon)] d\varepsilon, \\
&= -v_s \ln[1 + \exp(\zeta + v_s)] + \int_0^{\infty} \ln[1 + \exp(\zeta + v_s - \varepsilon'')] d\varepsilon'', \\
&= -v_s \ln[1 + \exp(\zeta + v_s)] + \Phi(\zeta + v_s), \\
\Phi(\zeta + v_s) &= \int_0^{\exp(\zeta + v_s)} \frac{\ln[1 + \Omega]}{\Omega} d\Omega, \quad I_2 = \int_{-v_s}^{\infty} \varepsilon^2 [1 + \exp(\varepsilon - \zeta)]^{-1} d\varepsilon \\
&= \{-\varepsilon^2 \ln[1 + \exp(\zeta - \varepsilon)]\}_{-v_s}^{\infty} + 2 \int_{-v_s}^{\infty} \varepsilon \ln[1 + \exp(\zeta - \varepsilon)] d\varepsilon \\
&= v_s^2 \ln[1 + \exp(\zeta + v_s)] + 2 \int_{-v_s}^{\infty} \varepsilon \ln[1 + \exp(\zeta - \varepsilon)] d\varepsilon \\
&= v_s^2 \ln[1 + \exp(\zeta + v_s)] + 2 \int_0^{\infty} (-v_s + \varepsilon_1) \ln[1 + \exp(\zeta - \varepsilon_1 + v_s)] d\varepsilon_1 \\
&= v_s^2 \ln[1 + \exp(\zeta + v_s)] - 2v_s \Phi(\zeta + v_s) + 2I_3(\zeta + v_s).
\end{aligned} \tag{2.72b}$$

and

$$I_3(\Omega) = \int_0^{\infty} \eta \ln[1 + \exp(\Omega - \eta)] d\eta. \tag{2.73c}$$

Thus, the mean energy far away from the surface is given by

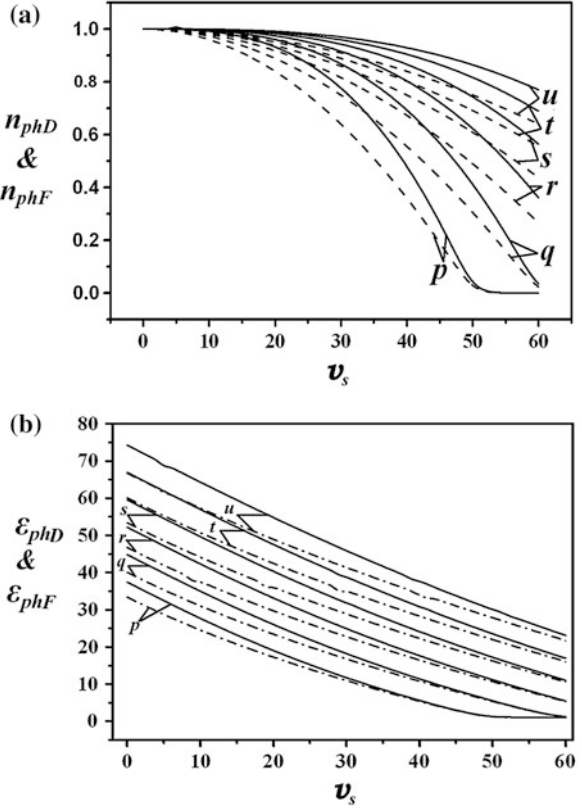
$$\varepsilon_{\text{ph}} = \varepsilon_{\text{ph}0} + v_s = \frac{-v_s \Phi(\zeta + v_s) + 2I_3(\zeta + v_s)}{\Phi(\zeta + v_s) - v_s \ln[1 + \exp(\zeta + v_s)]}.$$

If n_p denotes the rate of photoelectron emission from an uncharged surface ($-v_s = 0$)

$$[n_{\text{ph}}/n_p] = I_1(\zeta, -v_s)/\Phi(\zeta). \tag{2.72c}$$

Many investigators have used the intuitive and erroneous relation

Fig. 2.13 Dependence of rate of emission (n_{phD}/n_{ph0}), (n_{phF}/n_{ph0}) and mean energy ϵ_{phD} , ϵ_{phF} of emitted photoelectrons on the electric potential $v_s (= -eV_s/kT)$ at the surface of an emitting spherical particle; the continuous and broken curves refer to Du-Bridge and Fowler theories respectively, while the letters p , q , r , s , t and u refer to equal to $\xi = 50, 60, 70, 80, 90$, and 100 , respectively (after Misra et al. [30], curtsey authors and publishers NRC Press)



$$(n_{ph}/n_p) = \exp(v_s). \quad (2.72d)$$

Misra and Sodha [30] have evaluated (n_{ph}/n_p) and ϵ_{ph} on the basis of modified DuBridge theory; the v_s dependence of the both the parameters corresponding to Fowler's and modified DuBridge theory is shown in Fig. 2.13a, b.

It is seen from Fig. (2.14) that the disagreement between the correct (2.72c) and erroneous (2.72d) increases with increasing ξ and $-v_s$. Since for most situations of interest ξ is large, the use of (2.72d) can lead to unacceptably large errors.

In Tables 2.6a, b, c, and 2.7a, b, c n_{ph}/n_p and ϵ_{ph} have been tabulated as functions of ξ and $-v_s$ (after Sodha et al. [44], curtsey authors and publishers APS)

2.8.3.5 Cylindrical Surface

We consider emission from an element of the surface, normal to x direction and assume the z axis to be along the axis of the cylindrical surface; the potential energy of an electron at the surface is $-V_s$ (Sodha et al. [49]).

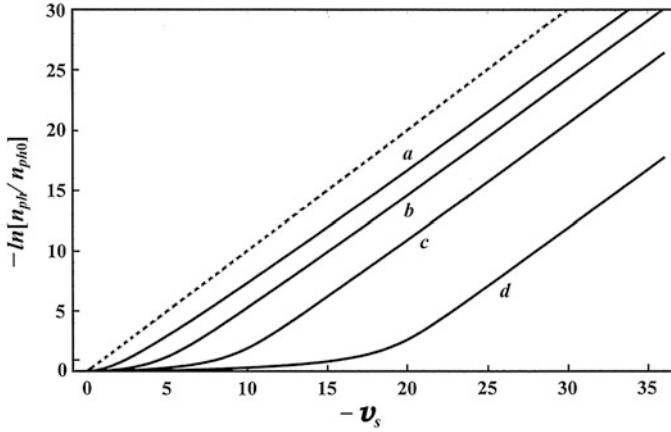


Fig. 2.14 Dependence of n_{ph}/n_p on $-v_s$ for different values of ζ . The *solid curves a, b, c, d* refer to (2.59c) and $\zeta = 5, 10, 15$, and 20 . The *broken straight line* refer to the erroneous (2.59d) (after Misra et al. [29], courtesy authors and publishers Springer)

2.8.3.6 Thermionic Emission

From (2.8a) and (2.8c), the number of electrons incident per unit area per unit time on an element of the surface, normal to the x direction is

$$d^3n_1 = (p_x/m_e)(2/h^3)F_D[(p^2/2m_e k_B T) - (E_F/k_B T)]dp_x dp_y dp_z. \quad (2.8d)$$

For electrons of interest to thermionic emission $p_x^2/2m_e > W_a$ and the above equation reduces to (see the argument after (2.33)).

$$d^3n_1 = (p_x/m_e)(2/h^3) \exp(E_F/k_B T) \exp[-(p_x^2 + p_y^2 + p_z^2/2m_e k_B T)]dp_x dp_y dp_z \quad (2.8e)$$

If p' denotes the electron momentum just outside the surface

$$(p_x'^2/2m_e) = (p_x^2/2m_e) - W_a, p_y' = p_y \text{ and } p_z' = p_z.$$

The momentum distribution of electrons just outside the surface element is thus

$$d^3n_{th} = (p_x'/m_e)(2/h^3) \exp(-\Phi/k_B T) \exp[-(p_x'^2 + p_y'^2 + p_z'^2/2m_e k_B T)]dp_x' dp_y' dp_z' \quad (2.8f)$$

where Φ is the work function of the metal.

As discussed before (47c) only those electrons get emitted for which $(p_x'^2 + p_y'^2)/2m_e > -V_s$; thus the number of electrons, emitted per unit area from the surface can be obtained by integrating (3f), subject to this inequality. Hence,

Table 2.6 n_{ph}/n_p for $1 < \xi < 300$

$\xi \rightarrow$ $\downarrow (-v_S)$	1	2	3	4	5	6	7	8
1	1.73234	1.96651	2.30933	2.74097	3.261	3.77477	4.34342	4.93313
2	1.43231	1.56106	1.79139	2.12938	2.55559	3.04494	3.57764	4.14028
3	1.28821	1.34624	1.47161	1.69632	2.02678	2.44437	2.92464	3.44821
4	1.21417	1.23733	1.29404	1.41665	1.63662	1.9605	2.37022	2.84195
5	1.17184	1.18058	1.20332	1.25902	1.37946	1.59565	1.91414	2.31726
6	1.14474	1.14796	1.15657	1.17899	1.23388	1.35262	1.56579	1.87989
7	1.12569	1.12686	1.13004	1.13855	1.16071	1.21497	1.33234	1.54306
8	1.11136	1.11179	1.11296	1.11611	1.12453	1.14648	1.20022	1.31647
9	1.10009	1.10025	1.10067	1.10183	1.10496	1.11331	1.13509	1.1884
10	1.09094	1.091	1.09116	1.09158	1.09273	1.09583	1.10413	1.12576
$\xi \rightarrow$ $\downarrow (-v_S)$	9	10	15	20	30	40	50	60
1	5.53803	6.15411	9.33055	12.5829	19.1673	25.7922	32.4375	39.0876
2	4.72408	5.32328	8.44792	11.6733	18.2294	24.8397	31.4746	38.1173
3	4.00191	4.57712	7.62838	10.8145	17.3283	23.916	30.533	37.1653
4	3.35671	3.9016	6.86264	10.0005	16.4609	23.0191	29.617	36.2363
5	2.78163	3.2886	6.1435	9.22611	15.6242	22.1474	28.7248	35.33
6	2.27754	2.73567	5.46544	8.487	14.8159	21.2993	27.8512	34.4406
7	1.85357	2.24665	4.82446	7.7796	14.0335	20.4731	26.9949	33.5633
8	1.52518	1.8327	4.21803	7.10093	13.2752	19.6676	26.1574	32.6998
9	1.30372	1.51075	3.64525	6.4486	12.5391	18.8816	25.338	31.8541
10	1.17871	1.29325	3.1074	5.82069	11.8237	18.138	24.5343	31.0262
$\xi \rightarrow$ $\downarrow (-v_S)$	70	80	90	100	150	200	250	300
1	45.7381	52.3544	58.9834	65.8947	98.2935	131.018	166.614	198.15
2	44.7672	51.3854	58.0506	64.8368	97.2761	130.446	165.765	199.011
3	43.812	50.4415	57.1345	63.8029	96.352	129.744	164.54	199.884
4	42.8736	49.5158	56.2234	62.7946	95.4268	128.576	162.82	200.395
5	41.9518	48.5982	55.3038	61.8123	94.5055	127.428	161.362	199.966
6	41.0457	47.6824	54.369	60.8548	93.6061	126.829	160.658	197.953
7	40.154	46.7712	53.4304	59.9208	92.7189	126.483	160.325	194.689
8	39.2759	45.8728	52.4999	59.009	91.8461	125.745	159.643	191.947
9	38.4125	44.9915	51.587	58.1178	90.981	124.464	158.073	190.827
10	37.564	44.1268	50.6945	57.2456	90.1328	123.327	155.97	190.958

Table 2.7 ε_{ph} for $1 < \xi < 300$

$\xi \rightarrow$ $\downarrow (-v_S)$	1	2	3	4	5	6	7	8
1	0.839078	0.887760	0.925374	0.949896	0.965100	0.974670	0.980910	0.985150
2	0.534340	0.628570	0.727196	0.806901	0.862410	0.899220	0.92379	0.940640
3	0.283342	0.363810	0.476054	0.059689	0.699856	0.775940	0.829300	0.866660
4	0.134824	0.181770	0.261115	0.373447	0.499309	0.612023	0.699590	0.763850
5	0.060334	0.083130	0.125604	0.197883	0.303306	0.426250	0.541180	0.634240
6	0.026030	0.036170	0.05589	0.09272	0.156890	0.253600	0.370480	0.483750
7	0.010965	0.015290	0.023833	0.040439	0.072110	0.128878	0.217050	0.326920
8	0.004541	0.006340	0.009916	0.016977	0.030970	0.058365	0.108810	0.189260
9	0.001856	0.002590	0.004061	0.006977	0.012843	0.024766	0.048710	0.093860
10	0.00075	0.001050	0.001645	0.002829	0.00523	0.010168	0.020470	0.041620
$\xi \rightarrow$ $\downarrow (-v_S)$	9	10	15	20	30	40	50	60
1	0.988129	0.99033	0.995620	0.99752	0.998890	0.999400	0.999460	0.999660
2	0.952560	0.96128	0.982480	0.990080	0.995570	0.997520	0.998300	0.998880
3	0.893337	0.91290	0.960580	0.977680	0.990040	0.994400	0.996430	0.997630
4	0.810651	0.84524	0.929910	0.960330	0.982290	0.990030	0.993650	0.995700
5	0.705120	0.75848	0.890490	0.938010	0.972320	0.984420	0.989970	0.993080
6	0.578649	0.65322	0.842320	0.910730	0.960150	0.977560	0.985550	0.959920
7	0.436643	0.53124	0.785380	0.878500	0.09458	0.969450	0.980400	0.986350
8	0.292142	0.39751	0.719710	0.841310	0.929150	0.960100	0.974430	0.982320
9	0.167535	0.26383	0.645360	0.799150	0.910330	0.949490	0.967600	0.977660
10	0.082364	0.15014	0.562490	0.752040	0.889290	0.937640	0.960000	0.972290
$\xi \rightarrow$ $\downarrow (-v_S)$	70	80	90	100	150	200	250	300
1	0.999711	1.00000	0.99929	1.00100	0.999950	0.999120	1.001030	0.998600
2	0.999060	0.99944	0.99815	1.001800	0.999720	0.998130	1.002010	0.997160
3	0.998056	0.99834	0.99666	1.002380	0.999320	0.997050	1.002910	0.995680
4	0.996600	0.99684	0.99502	1.002550	0.998740	0.995870	1.003750	0.994150
5	0.994800	0.99513	0.99351	1.002340	0.997980	0.994590	1.004530	0.992570
6	0.992550	0.99337	0.99227	1.001730	0.997050	0.993210	1.005240	0.990950
7	0.989900	0.99152	0.99117	1.000720	0.995940	0.991730	1.005890	0.989290
8	0.986878	0.98937	0.98993	0.999310	0.994660	0.990150	1.006470	0.987580
9	0.983410	0.98681	0.98836	0.997510	0.993200	0.988471	1.006990	0.985830
10	0.979486	0.98382	0.98636	0.995300	0.991560	0.986710	1.007450	0.984030

$$\begin{aligned}
n_{\text{th}} &= (2/m_e h^3) \exp(-\varphi) \left[\int_{-\infty}^{\infty} \exp(-p_z'^2/2m_e k_B T) dp_z' \right] \\
&\times 2 \left\{ \left\{ \int_{p_y'=0}^{p_0} \int_{p_x'=(p_0^2-p_y'^2)^{1/2}}^{\infty} p_x' \exp[-(p_x'^2 + p_y'^2)/2m_e k_B T] dp_x' dp_y' \right\} \right\} \\
&+ \left\{ \left\{ \int_{p_y'=p_0}^{\infty} \int_{p_x'=0}^{\infty} p_x' \exp[-(p_x'^2 + p_y'^2)/2m_e k_B T] dp_x' dp_y' \right\} \right\} \\
&= (4\pi m_e k_B^2 T^2/h^3) \exp[-\varphi + v_s] \cdot \{ (2/\sqrt{\pi})(-v_s)^{1/2} + \exp[-v_s] \text{erfc}((-v_s)^{1/2}) \} \\
&\hspace{15em} (2.73e)
\end{aligned}$$

where $\varphi = (W_a - E_F)/k_B T$, $p_0^2/2m_e = -V_s$, $v_s = V_s/k_B T$ and $\text{erfc}(\eta) = (2/\sqrt{\pi}) \int_{\eta}^{\infty} \exp[-t^2] dt$.

The factor 2 in (2.73e) is on account of the fact that p_y' varies between $-\infty$ to $+\infty$. The corresponding mean energy of the electrons far away from the surface of the particle can be shown [43] to be given by

$$\varepsilon_{\text{th, far away}} = 2 + \frac{v_s \exp(-v_s) \text{erfc}((-v_s)^{1/2})}{(2/\sqrt{\pi})(-v_s)^{1/2} + \exp(-v_s) \text{erfc}((-v_s)^{1/2})} \quad (2.73f)$$

The dependence of the rate of thermionic emission $n_{\text{th}}/n_{\text{th0}}$ (subscript 0 refers to the uncharged surface) and mean electron energy ε_{th} far away from the surface on $-v_s$ is shown in Figs. 2.15 and 2.16 respectively.

It is seen that for a given value of the surface potential $-v_s$, $n_{\text{th}}/n_{\text{th0}}$ is higher for the spherical surface case, as compared to the cylindrical one. This is because the inequality (47c) allows more electrons to be emitted as compared to the case of inequality (47b).

It may also be noted that for a given value of $-v_s$ the mean energy of emitted electrons is higher in case of the cylindrical surface than in the case of spherical surface. This is because of the inequalities (47b) and (47c), which restrict three and two components of the momentum in the two cases.

2.8.3.7 Photoelectric Emission

If A photons of frequency ν are incident per unit area per unit time on the surface element and β is the probability of absorption of a photon, which would increase the normal energy of an electron incident on the surface, then the distribution of momenta \mathbf{p}' of electrons incident on the surface per unit area per unit time which

Fig. 2.15 Dependence of the rate of thermionic emissions (n_{th}/n_{th0}) on the surface potential ($-v_s$); *solid* and *broken* curves refer to cylindrical and spherical particles, respectively (after Sodha et al. [49], curtesy authors and publishers AIP)

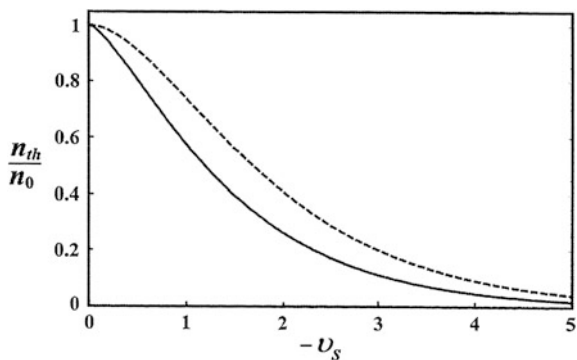
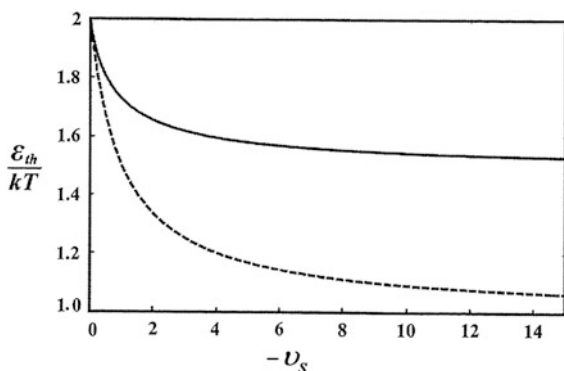


Fig. 2.16 Dependence of the mean energy of thermionically emitted electrons at a large distance from the dust particle, (ϵ_{th}) on the surface potential ($-v_s$); *solid* and *broken* curves corresponds to cylindrical and spherical particles respectively (after Sodha et al. [49], curtesy authors and publishers AIP)



have the normal energy enhanced by absorption of a photon can using (3d) be written down as:

$$d^3n_1 = \beta A(2/h^3)(p'_x/m_e)F_D[(p'^2/2m_e k_B T) - (hv/k_B T) - E_F/k_B T] dp'_x dp'_y dp'_z,$$

where $p'^2/2m_e = p^2/2m_e + hv$, $p'^2_x/2m_e = p^2_x/2m_e + hv$, $p'_y = p_y$, $p'_z = p_z$.

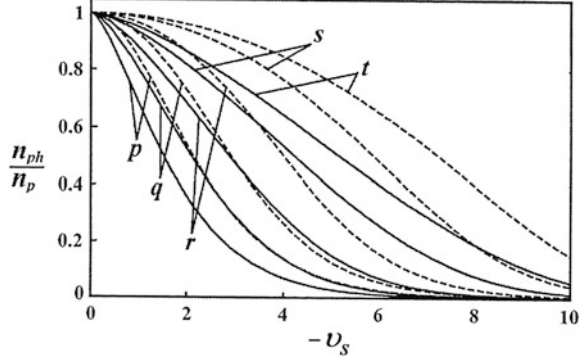
Hence, the momentum \mathbf{p}'' distribution of the electrons, outside the surface is given by

$$\begin{aligned} d^3n_{ph} &= \beta A(2/h^3)(p''_x/m_e)F_D[(p''^2/2m_e k_B T) + (W_a/k_B T) - (hv/k_B T) - E_F/k_B T] dp''_x dp''_y dp''_z \\ &= \beta A(2/h^3)(p''_x/m_e)F_D[(p''^2/2m_e k_B T) - \xi] dp''_x dp''_y dp''_z, \end{aligned} \quad (2.74)$$

where $p''^2_x = p^2_x - W_a$, $p''_y = p_y$, $p''_z = p_z$ and $\xi = (hv - \Phi)/k_B T$.

Proceeding as in the case of thermionic emission, the number of emitted photoelectrons per unit area per unit time from the surface and corresponding mean energy far away from the particle is given by

Fig. 2.17 Dependence of photoelectric emission rate of electrons (n_{ph}/n_p) on the surface potential ($-v_s$). The letters p , q , r , s and t on the curves refer to $\xi = 1, 3, 5, 8$ and 10 respectively; *solid* and *broken* curves correspond to cylindrical and spherical particles, respectively (after Sodha et al. [49], curtsey authors and publishers AIP)



$$\begin{aligned}
 n_{ph} = \iiint d^3 n_{ph} = & \beta A (8 m_e k_B^2 T^2 / h^3) \times \{ (-v_s)^{1/2} \int_{\xi_3=0}^{\infty} (\xi_3)^{-1/2} \times \ln\{1 + \exp[\xi + v_s - \xi_3]\} d\xi_3 \\
 & + \frac{1}{2} \int_{\xi_3=0}^{\infty} \int_{\xi_2=-v_s}^{\infty} (\xi_2 \xi_3)^{-1/2} \times \ln\{1 + \exp[\xi - \xi_2 - \xi_3]\} d\xi_2 d\xi_3 \},
 \end{aligned} \quad (2.75a)$$

where

$$\xi_2 = p_x''^2 / 2m_e k_B T \quad \text{and} \quad \xi_3 = p_z''^2 / 2m_e k_B T. \quad (2.75b)$$

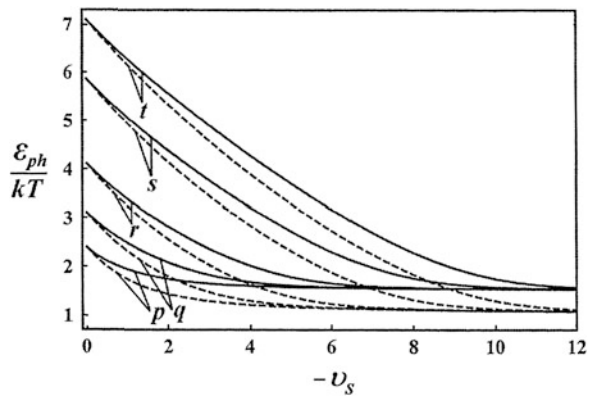
$$\frac{\varepsilon_{ph}^I}{k_B T} = \frac{\varepsilon_{ph}}{k_B T} + v_s, \quad (2.75c)$$

and

$$\begin{aligned}
 n_{ph}(\varepsilon_{ph}/k_B T) = & \beta A (8 m_e k_B^2 T^2 / h^3) \times \{ (-v_s)^{1/2} \int_{\xi_3=0}^{\infty} (\xi_3)^{-1/2} [\xi_3 - v_s] \times \ln\{1 + \exp[-\{-v_s + \xi_3 - \xi\}]\} d\xi_3 \\
 & + (1/2) \int_{\xi_3=0}^{\infty} \int_{\xi_2=0}^{ev} \int_{\xi_1=-v_s-\xi_2}^{\infty} (\xi_2 \xi_3)^{-1/2} \times \ln\{1 + \exp[-(\xi_1 + \xi_2 + \xi_3 - \xi)]\} d\xi_1 d\xi_2 d\xi_3 \\
 & + (1/2) \int_{\xi_3=0}^{\infty} \int_{\xi_2=-v_s}^{\infty} (\xi_2 \xi_3)^{-1/2} (\xi_2 + \xi_3) \times \ln\{1 + \exp[-(\xi_2 + \xi_3 - \xi)]\} d\xi_2 d\xi_3 \\
 & + (1/2) \int_{\xi_3=0}^{\infty} \int_{\xi_2=-v_s}^{\infty} \int_{\xi_1=0}^{\infty} (\xi_2 \xi_3)^{-1/2} \times \ln\{1 + \exp[-(\xi_1 + \xi_2 + \xi_3 - \xi)]\} d\xi_1 d\xi_2 d\xi_3 \}
 \end{aligned} \quad (2.76)$$

The dependence of the rate of photoelectric emission and the mean energy of photoelectrons far away from the surface on the surface potential is illustrated in Figs. 2.17 and 2.18.

Fig. 2.18 Dependence of the mean energy of the photoelectrons (at a large distance from the dust grains), (ϵ_{ph}) on the surface potential ($-v_s$). The letters p , q , r , s and t on the curves refer to the $\xi = 1, 3, 5, 8$ and 10 respectively; *solid* and *dotted* curves correspond to cylindrical and spherical particles respectively (after Sodha et al. [49], courtesy authors and publishers AIP)



2.8.4 Transmission Coefficient for Electrons

2.8.4.1 Negatively Charged Surfaces

For the study of electric field emission of electrons from curved surfaces it is usual to utilize the result for a plane surface and substitute the electric field at the surface for the constant electric field in the case of a plane surface. Almost all efforts in the case of curved surfaces are limited to the case of electric field emission; the expressions for the transmission coefficient are applicable only for low values of electron energy (above the bottom of the conduction band), typically up to half of the height of the surface potential energy barrier W_a . Expressions for the transmission coefficient (corresponding to electric field emission) in case of spherical and cylindrical surfaces were obtained in the *Born approximation* by [45, 47] by solving Schrödinger's equation for the appropriate unshielded electric potential, in the JWKB approximation. Dubey [10] conducted a similar analysis with the inclusion of the image force. Sodha et al. [42, 43] obtained appropriate expressions in the case of spherical and cylindrical surfaces respectively, employing the formalism by Ghatak et al. [16, 35] and using the three-region model of electron potential energy variation in the vicinity of the surface. In this section, an analysis (Sodha et al. [44]) for spherical and cylindrical cases, using appropriate expressions, corresponding to *Debye-Huckel* shielding has been presented. It may be mentioned that Prakash [34] has made an analysis, corresponding to nonlinear shielding. However, the formalism adopted so far is valid only for low energy (less than that corresponding to $0.5 W_a$) and a more rigorous treatment is required. A fairly rigorous treatment, applicable to all values of electron energy has been given by Mishra et al. [28], which is outlined in what follows.

2.8.4.2 Spherical Surface

The electron potential energy $V(r)$ in and out of a spherical particle of radius a , charged to an electric potential $(-V_s/e)$, corresponding to the electron potential energy V_s at the surface is given by [28]

$$V(r) = V_s - W_a \quad \text{for } r < a \quad (\text{Region-I})$$

and

$$V(r) = (aV_s/r)\exp[-(r-a)/\lambda_D] \quad \text{for } r > a \quad (\text{Region-II})$$

where W_a is the height of the surface electron potential energy barrier of the material of the particle,

λ_D is the Debye length in the plasma and

$-e$ is the electronic charge.

It is convenient for purposes of computation to express the potential energy in a dimensionless form as follows and have another Region-III ($r > r_n$), such that $V(r)$ in this region is very nearly zero (say $<0.05 V_s$).

Thus,

$$v(\rho) = (v_s - 1) \quad \text{for } \rho < 1 \quad (\text{Region-I}) \quad (2.77a)$$

$$v(\rho) = (v_s/\rho) \exp[-(\rho - 1)/\mu_d] \quad \text{for } 1 < \rho < \rho_n \quad (\text{Region-II}) \quad (2.77b)$$

and

$$v(\rho) = 0 \quad \text{for } \rho > \rho_n \quad (\text{Region-III}) \quad (2.77c)$$

where $v(\rho) = (V(r)/W_a)$, $v_s = (V_s/W_a)$, $\rho = (r/a)$, $\mu_d = (\lambda_D/a)$ and $\rho_n = (r_n/a)$.

2.8.4.3 Schrödinger's Equation

Putting

$$\psi(r, \theta, \varphi) = r\psi(r)Y_{l,m}(\theta, \varphi),$$

(as is the case for a spherically symmetrical potential energy) and interpreting the orbital quantum number l semiclassically, *Schrödinger's* equation, corresponding to an electron in a spherically symmetric potential reduces [28] to

$$\frac{d^2\psi}{dr^2} + \frac{8\pi^2m_e}{h^2}(E_r - V(r))\psi = 0$$

or

$$\frac{d^2\psi}{d\rho^2} + \beta(e_r - V(\rho))\psi = 0, \quad (2.78)$$

where $\beta = (8\pi^2 m_e a^2 W_a / h^2)$, $e_r = (E_r / W_a)$ and E_r is the radial kinetic energy of an electron due to the radial component of its momentum in Region-III, where $V(r) = 0$; hence is also the total (kinetic plus potential) energy of the electron.

Substituting for $V(\rho)$ from (2.77a), (2.77b) and (2.77c) in (2.78), *Schrödinger's* equation in the three regions may be expressed as:

$$\frac{d^2\psi}{d\rho^2} + \beta(e_r - v_s + 1)\psi = 0 \quad \text{for } \rho < 1 \text{ (Region-I),} \quad (2.79a)$$

$$\frac{d^2\psi}{d\rho^2} + \beta\{e_r - (v_s/\rho) \exp[-(\rho - 1)/\mu_d]\}\psi = 0 \quad \text{for } 1 < \rho < \rho_n \text{ (Region-II)} \quad (2.79b)$$

and

$$\frac{d^2\psi}{d\rho^2} + \beta e_r \psi = 0 \quad \text{for } \rho > \rho_n \text{ (Region-III).} \quad (2.79c)$$

The tangential component of the momentum is not affected by the movement of the electron in the three regions; hence, the radial kinetic energy inside the particle $e'_r = E'_r / W_a$ is given by

$$e'_r + v_s - 1 = e_r + 0 \quad \text{(Region-I) (Region-III)}$$

or

$$e'_r = e_r - v_s + 1. \quad (2.80)$$

For computation ρ_n is obtained by putting $\rho = \rho_n$ and $v(\rho = \rho_n) = 0.05 v_s$ in (2.77b).

The interval $1 < \rho < \rho_n$ is divided in n segments where the q th segment is defined by $(1 + q\delta) < \rho < (1 + (q + 1)\delta)$ and $\delta = (\rho_n - 1)/n$.

The electron potential energy $v(\rho)$ in the q th segment of the second region may be approximated as

$$v_q(\rho) = v(1 + q\delta) + [\rho - (1 + q\delta)]\{v[1 + (1 + q)\delta] - v(1 + q\delta)\}\delta^{-1}, \quad (2.80d)$$

where q varies from zero to $(n - 1)$ and $v(\rho)$ is given by (2.77b).

Equation (2.80d) implies that v_s in a segment varies linearly with r and is not uniform.

In other words, (2.80d) is an improvement over the usual assumption

$$v_q(\rho) = [v(1 + q\delta) + v(1 + (1 + q)\delta)]/2,$$

which has not been used herein; this assumption is usually made in such situations.

The usual boundary conditions are the continuity of ψ and its derivative at the interfaces of regions/segments.

2.8.4.4 General Solution of *Schrödinger's Equation*

The general solution in Region-I (inside the particle), Region-II (q th Segment), and Region-III (far away from the particle) may from (2.79a), (2.79b) and (2.79c) be expressed as:

$$\text{Region-I: } \psi(\rho) = A \exp[ik_1(\rho - 1)] + B \exp[-ik_1(\rho - 1)], \quad (2.81a)$$

$$\text{Region-II: } \psi(\rho) = C_q Ai[\eta_q] + D_q Bi[\eta_q] \quad (2.81b)$$

and

$$\text{Region-III: } \psi(\rho) = E \exp[ik_3(\rho - \rho_n)] + F \exp[-ik_3(\rho - \rho_n)], \quad (2.81c)$$

where

$$k_1^2 = \beta(\varepsilon_r - v_s + 1), \eta_q = -(\varepsilon_r - v_q(\rho))/f_q^{2/3},$$

$$f_q = \beta v_s \exp(-q\delta/\mu_d) \frac{1}{\delta} \left(\frac{\exp(-\delta/\mu_d)}{[1+(q+1)\delta]} - \frac{1}{[1+q\delta]} \right) \text{ and } k_3^2 = \beta\varepsilon_r.$$

2.8.4.5 Transmission of Electrons

When electron emission is considered

$$F = 0, \quad A = 1 \quad (\text{arbitrary}) \quad (2.81d)$$

and when electron accretion is considered

$$A = 0, \quad F = 1 \quad (\text{arbitrary}). \quad (2.81e)$$

The transmission coefficient $F = 1$ (arbitrary) in the two cases is given by

$$D_e = 1 - BB^*/AA^* \quad (\text{Emission}) \quad (2.82a)$$

and

$$D_a = 1 - EE^*/FF^* \quad (\text{Accretion}) \quad (2.82b)$$

the subscripts e and a indicate emission and accretion respectively.

The coefficient A, B, C_q, D_q, E, F [q varying from zero to $(n - 1)$] may be obtained from the fact that ψ and $(d\psi/d\rho)$ are continuous at the interface of segments and region viz at $\rho = 1, \rho = 1 + (q + 1)\delta$ ($0 \leq q \leq (n - 1)$) and $\rho = \rho_n = (1 + n\delta)$. Thus

(i) at $\rho = 1$,

$$A + B = C_1 Ai[\eta_1] + D_1 Bi[\eta_1] \quad (2.83a)$$

and

$$ik_1(A - B) = f_1^{(1/3)}(C_1 Ai'[\eta_1] + D_1 Bi'[\eta_1]); \quad (2.83b)$$

(ii) at $\rho = 1 + (q + 1)\delta$ where $(0 \leq q \leq (n - 1))$,

$$C_q Ai[\eta_q] + D_q Bi[\eta_q] = C_{q+1} Ai[\eta_{q+1}] + D_{q+1} Bi[\eta_{q+1}] \quad (2.83c)$$

and

$$f_q^{1/3}(C_q Ai'[\eta_q] + D_q Bi'[\eta_q]) = f_{q+1}^{1/3}(C_{q+1} Ai'[\eta_{q+1}] + D_{q+1} Bi'[\eta_{q+1}]). \quad (2.83d)$$

(iii) at $\rho = \rho_n (= 1 + n\delta)$,

$$C_{\rho_n} Ai[\eta_{\rho_n}] + D_{\rho_n} Bi[\eta_{\rho_n}] = E + F, \quad (2.83e)$$

and

$$f_{\rho_n}^{1/3}(C_{\rho_n} Ai'[\eta_{\rho_n}] + D_{\rho_n} Bi'[\eta_{\rho_n}]) = ik_3(E - F). \quad (2.83f)$$

Thus, the transmission coefficients, corresponding to emission/accretion of electrons from/on a spherically negatively charged particle can be evaluated from (2.82a) and (2.82b), making use of (2.83a) to (2.83f) to obtain A , B , E , F .

In this section, the transmission coefficient for an electron having an arbitrary energy has been evaluated. This is in contrast to earlier work, applicable to electron energy e_r , which is less than half of the surface energy barrier.

For a better understanding of underlying physics and numerical appreciation of the results, three cases viz. (i) a spherical metallic particle at a temperature $T = 1500$ K, (thermionic and field emission) (ii) spherical metallic particle at a temperature $T = 300$ K, illuminated by a continuous source of monochromatic radiation causing photoemission, characterized by a parameter ξ and light induced field emission and (iii) accretion (classical as well as tunneling) of electrons at the surface of the spherical metallic particle, have been considered. Corresponding dependence of $D_e(e_r)$ and $D_a(e_r)$ on the radial energy of electrons e_r , potential energy at the surface and height of the surface energy barrier has been graphically illustrated. For computational purpose, the following standard sets of parameters have been used.

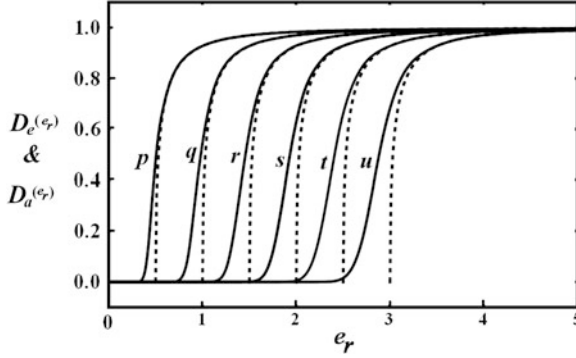


Fig. 2.19 Dependence of transmission coefficient [$D_e(e_r)$ or $D_a(e_r)$] on e_r for $\mu_d = (\lambda_D/a) = 5$ and $\beta = 1,000$. The labels on the curves p, q, r, s and t correspond to $v_s = 0.5, 1.0, 1.5, 2.0$ and 3.0 respectively. The *solid* curves correspond to the present analysis while the *dashed* curves refer to the step potential barrier of height $(1 - v_s)$ (after Mishra et al. [28], courtesy authors and publishers AIP)

2.8.4.6 For the Evaluation of Transmission Coefficient

$v_s = 0.5$, $\mu_d = (\lambda_D/a) = 5$ and $\beta = 1,000$.

2.8.4.7 For the Evaluation of Electron Currents

Case-I: $a = 10$ nm, $W_a = 10$ eV, $\mu_d = 5$ with $\phi = 5$ eV and $T = 1500$ K.

Case-II: $a = 10$ nm, $W_a = 10$ eV, $\mu_d = 5$ with $T = 300$ K.

Case-III: $a = 10$ nm, $W_a = 10$ eV, $\mu_d = 5$.

Parametric dependences have been investigated by varying one of these parameters, keeping others unchanged.

The set of Fig. 2.19 illustrates the dependence of the transmission coefficient [$D_e(e_r)$ and $D_a(e_r)$] on the radial energy of electrons e_r and e'_r corresponding to far away from and inside the particle as a function of v_s (surface potential) (Figs. 2.19, 2.20), parameter β (Fig. 2.21) and Debye length (μ_d) (Fig. 2.22).

It is seen from Fig. 2.19 that the transmission coefficient [i.e., $D(e_r)$] increases monotonically with increasing e_r and v_s , and approaches unity asymptotically for large e_r . In the curves the region $e_r < v_s$ is indicative of the contribution to the electron emission through tunneling (electric field emission) while the rest (i.e., $e_r > v_s$) corresponds to classically allowed emission; the broken curves correspond to transmission coefficient for step potential barrier [$D_0(e_r)$] corresponding to v_s (when W_a is substituted by $(W_a - V_s)$). The transmission coefficient corresponding to irradiated metallic particles (causing photoemission) may be obtained by shifting e_r -axis by $e_v (= hv)$. Further it is seen that the numerical values of the transmission coefficient, corresponding to accretion [$D_a(e_r)$] and emission [$D_e(e_r)$] of electrons are very close to each other and almost indistinguishable on the same graph.

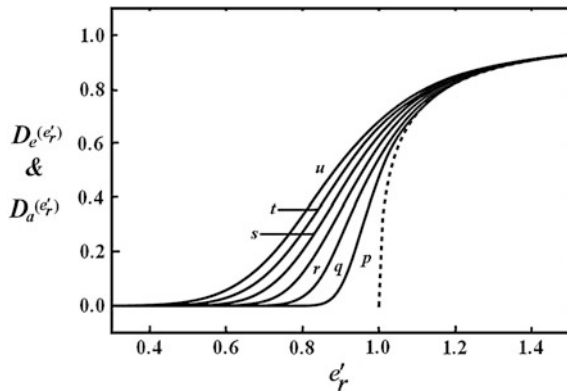


Fig. 2.20 Dependence of transmission coefficient $[D_e(e'_r) \text{ or } D_a(e'_r)]$ on e'_r for $\mu_d = (\lambda_D/a) = 5$ and $\beta = 1,000$. The labels on the curves p, q, r, s and t correspond to $v_s = 0.5, 1.0, 1.5, 2.0$ and 3.0 respectively. The *solid curves* correspond to the present analysis while the *dashed curves* refer to the step potential barrier of height $(1 - v_s)$ (after Mishra et al. [28], curtesy authors and publishers AIP)

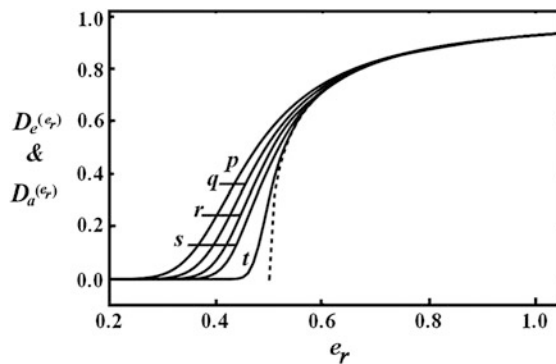


Fig. 2.21 b Dependence of transmission coefficient $[D_e(e_r) \text{ or } D_a(e_r)]$ on e_r for $v_s = 0.5$, and $\mu_d = (\lambda_D/a) = 5$. The labels on the curves p, q, r, s , and t correspond to $\beta = 250, 500, 1,000, 2,000$ and $26,000$ respectively. The *solid curves* correspond to the present analysis while the *dashed curves* refer to the step potential barrier of height $(1 - v_s)$ (after Mishra et al. [28], curtesy authors and publishers AIP)

The graphical representation for transmission of the set of Fig. 2.19 is well applicable to the latter two cases viz. irradiated particles and accretion. The fact that $D_e(e_r) \approx D_a(e_r)$ is the necessary and sufficient condition [48] for the validity of *Saha's equation* in thermal equilibrium of a system of electron emitting dust and electrons accreting on the surface of the particles. Since *Saha's equation* is based on statistical thermodynamics, without regard to process details, this result is a source of satisfaction. By the way this result relaxes the previous condition [48] for

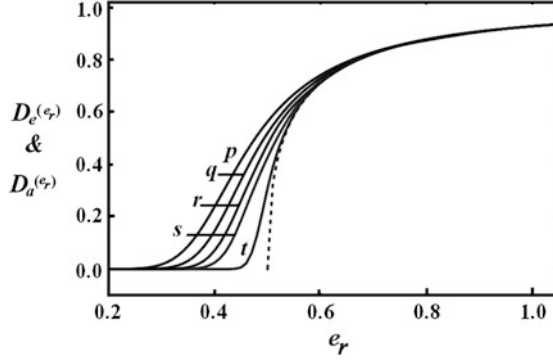


Fig. 2.22 Dependence of transmission coefficient [$D_e(e_r)$ or $D_a(e_r)$] on e_r for $v_s = 0.5$ and $\beta = 1,000$. The labels on the curves p , q , r , s and t correspond to $\mu_d = 5, 10, 20, 50$ and 100 respectively. The *solid curves* correspond to the present analysis while the *dashed curves* refer to the step potential barrier of height $(1 - v_s)$ (after Mishra et al. [28], courtesy authors and publishers AIP)

the validity of *Saha's equation* viz the applicability of *Born's approximation*. In what follows, the discussion is in terms of $D_e(e_r)$ and $D_a(e_r)$.

It is interesting to notice that contribution of the field emission and departure of $D(e_r)$ from $D_0(e_r)$ increases with increasing v_s while the converse is true with increasing $\beta(a \text{ \& } W_a)$ and μ_d ; the nature of dependence may be understood in terms of changing barrier width and has been displayed in Figs. 2.21 and 2.22. This behavior also underlines the fact that the contributions of pure thermionic or photoelectric emission currents get significantly enhanced with increasing v_s .

2.8.5 Electron Emission

2.8.5.1 Electron Emission Current

The number of electrons incident per unit area per unit time on an element of surface normal to x (as explained earlier) is

$$d^2n_1 = (A_0 T^2 / e) F_D[(\epsilon'_x + \epsilon'_t - \epsilon'_f)] d\epsilon'_x d\epsilon'_t. \quad (2.9a)$$

where $(A_0/e) = (4\pi m_e k_B^2 / h^3)$ and $A_0 = 120 \text{ A/cm}^2 \text{K}^2$.

Equation (2.9) is valid for all elements of a curved surface when the x direction is normal to it. For a spherical surface, it is convenient to replace ϵ'_x by ϵ'_r where r refers to radial. Thus,

$$d^2n_1 = (A_0 T^2 / e) F_D[(\epsilon'_r + \epsilon'_t - \epsilon'_f)] d\epsilon'_r d\epsilon'_t. \quad (2.9b)$$

It is important to remember that integration over ε'_t is equivalent to sum over l the orbital quantum number.

2.8.5.2 Dark Electron Emission Current (Thermionic and Electric Field Emission)

From (2.9b), the electron emission current n_t per unit area is given by

$$n_t = \int \int D_e(e_r)(A_0 T^2/e) F_D[(\varepsilon'_r + \varepsilon'_t - \varepsilon_f)] d\varepsilon'_r d\varepsilon'_t$$

and using (2.67)

$$n_t = \int \int D_e(\varepsilon'_r + v_s - 1)(A_0 T^2/e) F_D[(\varepsilon'_r + \varepsilon'_t - \varepsilon_f)] d\varepsilon'_r d\varepsilon'_t. \quad (2.84a)$$

The lower limit for ε'_r is given by $e_r = 0$ and hence it is $\varepsilon'_{rm} = 1 - v_s = 1 - (V_s/W_a)$ for $(V_s < W_a)$ and zero for $(V_s > W_a)$.

Hence, the electron emission current per unit area of the surface is given by

$$n_t = n_{th} + n_{fe},$$

where

$$n_{th} = (A_0 T^2/e) \int_g^\infty \int_0^\infty D_e(e'_r + v_s - 1) F_D[(\varepsilon'_r + \varepsilon'_t - \varepsilon_f)] d\varepsilon'_r d\varepsilon'_t \quad (2.84b)$$

and

$$n_{fe} = (A_0 T^2/e) \int_{ge'_{rm}}^g \int_0^\infty D_e(e'_r + v_s - 1) F_D[(\varepsilon'_r + \varepsilon'_t - \varepsilon_f)] d\varepsilon'_r d\varepsilon'_t, \quad (2.84c)$$

where n_{th} and n_{fe} correspond to thermionic ($E'_r > W_a$) and field emission ($E'_r < W_a$) and $g = (W_a/k_B T)$.

Substituting $\varepsilon'_r = g e'_{rm}$, $\varepsilon'_t = g e'_t$ and $\varepsilon_f = g e_f$ in the above two equations one obtains

$$n_{th} = (A_0/e) T^2 g^2 \int_1^\infty \int_0^\infty D_e(e'_r + v_s - 1) F_D[g(e'_r + e'_t - e_f)] d e'_r d e'_t \quad (2.85a)$$

$$n_{fe} = (A_0/e)T^2 g^2 \int_{e'_{rm}}^1 \int_0^\infty D_e(e'_r + v_s - 1) F_D[g(e'_r + e'_t - e_f)] de'_r de'_t. \quad (2.85b)$$

In case of thermionic emission one is interested only in electrons having an energy higher than W_a , which itself is much higher than the Fermi energy ($\gg k_B T$). Hence $\gamma = g(e'_x + e'_t - e'_f) \gg 1$ and $F_D(\gamma) = \exp(-\gamma)$.

Thus (2.72a) simplifies to

$$\begin{aligned} n_{th} &= (A_0/e)T^2 g^2 \exp(ge_f) \int_0^\infty \exp(-ge'_t) d\varepsilon'_t \int_1^\infty D_e(e'_r + v_s - 1) \exp(-ge'_r) de'_r \\ &= (A_0/e)T^2 g \exp(ge_f) \int_1^\infty D_e(e'_r + v_s - 1) \exp(-ge'_r) de'_r. \end{aligned} \quad (2.86)$$

If it is assumed as in many books and papers that $D_e = 1$, the above equation reduces to

$$n_{th0} = (A_0/e)T^2 \exp(-g + ge_f) = (A_0/e)T^2 \exp(-\phi/k_B T) \quad (2.87)$$

where $\Phi = W_a - E_F$ is the work function.

Equation (2.85b) can also be simplified by integrating with respect to e'_t . Thus,

$$n_{fe} = (A_0/e)T^2 g \int_{e'_{rm}}^1 D_e(e'_r + v_s - 1) \ln[1 + \exp[-g(e'_r - e_f)]] de'_r \quad (2.88)$$

The mean energy of emitted electron (inside the metal) e'_{th} and e'_{fe} are given by

$$e'_{th} = (A_0/en_{th})T^2 g^2 \int_1^\infty \int_0^\infty (e'_r + e'_t) D_e(e'_r + v_s - 1) F_D[g(e'_r + e'_t - e_f)] de'_r de'_t \quad (2.89)$$

$$e'_{fe} = (A_0/en_{fe})T^2 g^2 \int_{e'_{rm}}^1 \int_0^\infty (e'_r + e'_t) D_e(e'_r + v_s - 1) F_D[g(e'_r + e'_t - e_f)] de'_r de'_t \quad (2.90)$$

The mean energy of electrons far away from the particle is using (2.80) given by $e_{th} = e'_{th} + 1 - v_s$ and $e_{fe} = e'_{fe} + 1 - v_s$.

2.8.5.3 Photoelectric Current

(Photoelectric effect and light-Induced field emission)

The most widely used quantitative theory of photoelectric emission was formulated by [13], who assumed that the normal energy of a fraction $\beta(v)A(v)dv$ of the electrons incident on the surface from inside gets enhanced by an amount (hv) , when $A(v)dv$ photons of frequency between (v) and $(v + dv)$ are incident on the surface per unit area per unit time. Hence, the energy distribution of photoelectrons [whose normal energy has been enhanced by (hv)], incident per unit area per unit time from the inside is, using (2.9b), given by

$$d^2n_{ph} = \beta(v)A(v)dv(A_0T^2/e)F_D[(\varepsilon_r'' + \varepsilon_t'' - \varepsilon_v - \varepsilon_f)]d\varepsilon_r''d\varepsilon_t'', \quad (2.39)$$

where $\varepsilon_t'' = \varepsilon_t'$, $\varepsilon_r'' = \varepsilon_r' + (hv/k_BT)$ is the enhanced (after absorption of a photon) dimensionless radial energy and $e_v = hv/k_BT$.

Proceeding in the same way, as in the evaluation of dark electron current the total photoelectric current is using (2.79b), given by

$$n_{phT} = n_{ph}(v) + n_{life}(v), \quad (2.91a)$$

where

$$n_{ph}(v) = \int_{v_1}^{v_2} \beta(v)A(v)dv(A_0/e)T^2g \int_1^\infty D_e(e_r'' + v_s - 1) \ln[1 + \exp[-g(e_r'' - e_v - e_f)]]d\varepsilon_r'' \quad (2.91b)$$

and

$$n_{life}(v) = \int_{v_1}^{v_2} \beta(v)A(v)dv(A_0/e)T^2g \int_{\varepsilon_{rm}}^1 D_e(e_r'' + v_s - 1) \times \ln[1 + \exp[-g(e_r'' - e_v - e_f)]]d\varepsilon_r'' \quad (2.91c)$$

In case $D_e(e_r'') = 1$, (2.90) reduces to (2.41b) viz.

$$n_{ph0} = (A_0/e)T^2[\beta(v)A(v)]\Phi(\xi).$$

The corresponding mean energy of the emitted electrons while inside the particle is given by

$$n_{ph}\varepsilon_{ph}'' = \int_{v_1}^{v_2} \beta(v)A(v)dv(A_0/e)T^2g \int_1^\infty \int_0^\infty (e_r'' + e_t'')D_e(e_r'' + v_s - 1) (1 + \exp[g(e_r'' + e_t'' - e_v - e_f)])^{-1}d\varepsilon_r''d\varepsilon_t'' \quad (2.91d)$$

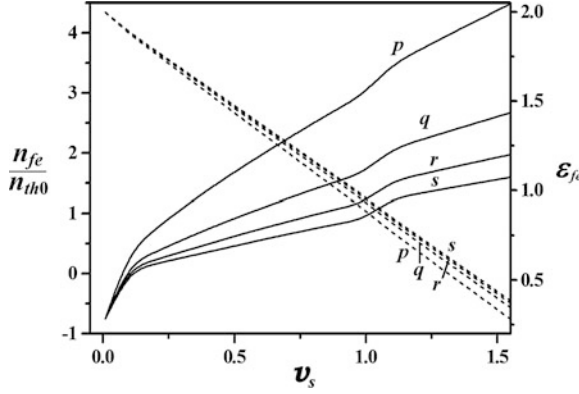


Fig. 2.23 Dependence of (n_{fe}/n_{th0}) and ϵ_{fe} with dimensionless surface potential (v_s), for Case-I $a = 10$ nm, $W_a = 10$ eV, $\mu_d = 5$ and $\Phi = 5$ eV. The labels on the curves p, q, r and s correspond to $T = 800, 1000, 1500$ K and 2000 K respectively. *Solid and broken lines* correspond to left and right hand scale respectively (after Mishra et al. [28], courtesy authors and publishers AIP)

$$n_{life} \epsilon''_{life} = \int_{v_1}^{v_2} \beta(v) A(v) dv (A_0/e) T^2 g \int_{e''_{m}}^1 \int_0^{\infty} (e''_r + e''_t) D_e(e''_r + v_s - 1) (1 + \exp[g(e''_r + e''_t - e_v - e_f)])^{-1} de''_r de_t \quad (2.91e)$$

The mean energy of electrons far away from the particle is using (2.80) given by $\epsilon_{ph} = \epsilon''_{ph} + 1 - v_s$ and $\epsilon_{life} = \epsilon''_{life} + 1 - v_s$.

2.8.5.4 Numerical Results and Discussion

The dependence of the electric field (n_{fe}/n_{th0}) and thermionic (n_{th}/n_{th0}) emission currents and associated respective mean energy (ϵ_{fe} and ϵ_{th} , far away from the particle surface) on the dimensionless surface potential (v_s) has been illustrated in the set of Fig. 2.23.

The figures indicate that the field emission currents are strongly influenced by surface potential and can largely contribute to the emission current (Figs. 2.23, 2.25) while thermionic emission also increases monotonically with v_s but with much slower rate than field emission (Figs. 2.24, 2.25-2.26). This behavior may be understood in terms of the availability of electrons for field emission inside metallic particles which is more than the availability of high energy electrons, corresponding to thermionic emission. The Figs. (2.23, 2.24) also display the fact that the thermionic emission current increases with increasing temperature of the spherical particle while field emission current displays the opposite trend; this may be ascribed to the large availability of electrons at high temperature for thermionic emission.

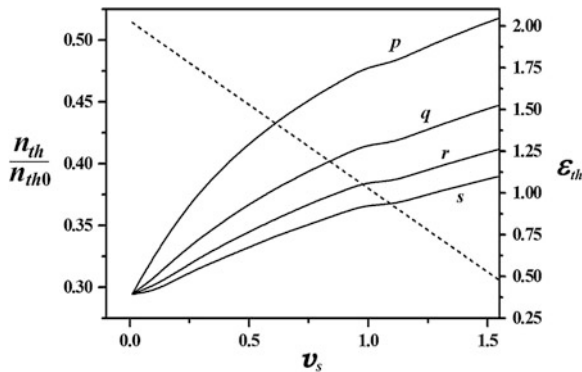


Fig. 2.24 Dependence of (n_{th}/n_{th0}) and ϵ_{th} with dimensionless surface potential (v_s), for Case-I $a = 10$ nm, $W_a = 10$ eV, $\mu_d = 5$ and $\Phi = 5$ eV. The labels on the curves p , q , r and s correspond to $T = 800, 1000, 1500$ and 2000 K respectively. Solid and broken lines correspond to left and right hand scale respectively (after Mishra et al. [28], courtesy authors and publishers AIP)

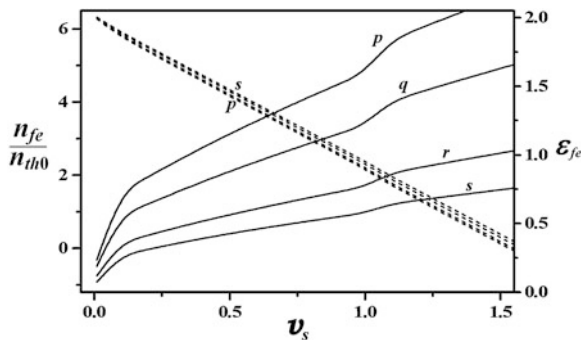


Fig. 2.25 Dependence of (n_{fe}/n_{th0}) and ϵ_{fe} with dimensionless surface potential (v_s), for Case-I, $T = 1500$ K, $W_a = 10$ eV, $\mu_d = 5$ and $\Phi = 5$ eV. The labels on the curves p , q , r and s correspond to $a = 5, 10, 15$ and 20 nm respectively. Solid and broken lines correspond to left and right hand scale respectively (after Mishra et al. [28], courtesy authors and publishers AIP)

Further, the size dependence has been illustrated in Figs. (2.25, 2.26) and can be understood in terms of $D(\epsilon_r)$ dependence on β which ensures the large contribution from field emission with smaller size (larger electric field for given (v_s)). Correspondingly the mean energy decreases with (v_s) on account of larger emission of low energy electrons with increasing surface potential (v_s); $\epsilon_{fe}/\epsilon_{th}$ display very weak dependence on size and temperature of the metallic particle.

The electron emission from spherical metallic particles in the presence of monochromatic radiation resulting in photoemission has been illustrated in Figs. 2.27, 2.28, 2.29. Figures 2.27 displays the dependence of light-induced field emission (n_{life}/n_{ph0}) and corresponding mean energy ϵ_{life} on surface potential (v_s) as

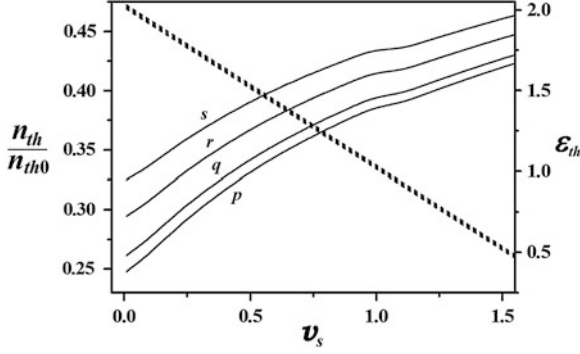


Fig. 2.26 Dependence of (n_{th}/n_{th0}) and ϵ_{th} with dimensionless surface potential (v_s), for Case-I, $T = 1500$ K, $W_a = 10$ eV, $\mu_d = 5$ and $\Phi = 5$ eV. The labels on the curves p , q , r and s correspond to $a = 5, 10, 15$ and 20 nm respectively. Solid and broken lines correspond to left and right hand scale respectively (after Mishra et al. [28], curtesy authors and publishers AIP)

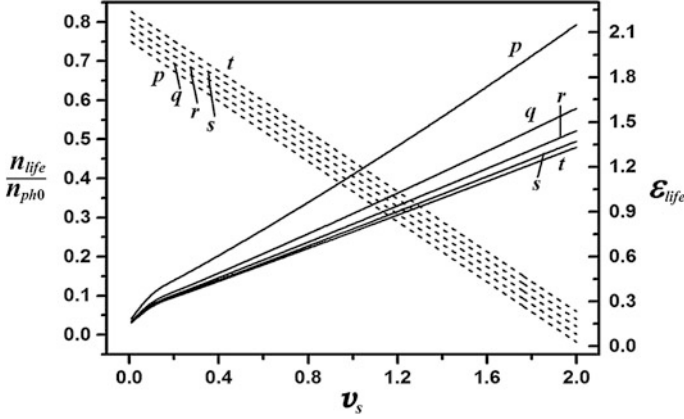


Fig. 2.27 Dependence of (n_{life}/n_{ph0}) and ϵ_{life} with dimensionless surface potential (v_s), for Case-II, $a = 10$ nm, $W_a = 10$ eV, $\mu_d = 5$ with $T = 300$ K. The labels on the curves p , q , r , s , and t correspond to $\xi = 0.1, 0.2, 0.3, 0.4$, and 0.5 , respectively. Solid and broken lines correspond to left and right hand scale, respectively (after Mishra et al. [28], curtesy authors and publishers AIP)

a function of the parameter $\xi [= g(\epsilon_v - \phi)]$, which usually characterizes the energy of the incident radiation and work function of the material. The figure suggests that n_{life}/n_{ph0} decreases with increasing ξ ; this behavior may be explained on the basis of the large availability of low energy electrons for the electric field emission. On the other hand, large availability of high energy electrons for photoemission (Fig. 2.28) explains the reverse trend for the ξ dependence of n_{ph}/n_{ph0} . Further the mean energy in both the cases increases with increasing ξ and may be understood in terms of emission of high energy electrons with increasing ξ . The

Fig. 2.28 Dependence of (n_{ph}/n_{ph0}) and ϵ_{ph} with dimensionless surface potential (v_s), for Case-II, $a = 10$ nm, $W_a = 10$ eV, $\mu_d = 5$ with $T = 300$ K. The labels on the curves p , q , r , s , and t correspond to $\xi = 0.1$, 0.2 , 0.3 , 0.4 , and 0.5 , respectively. Solid and broken lines correspond to left and right hand scale respectively (after Mishra et al. [28], courtesy authors and publishers AIP)

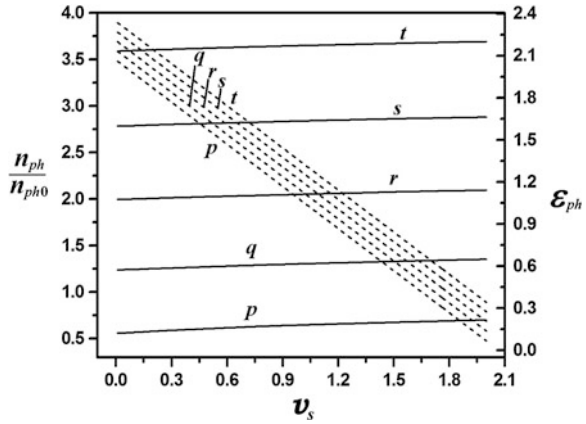
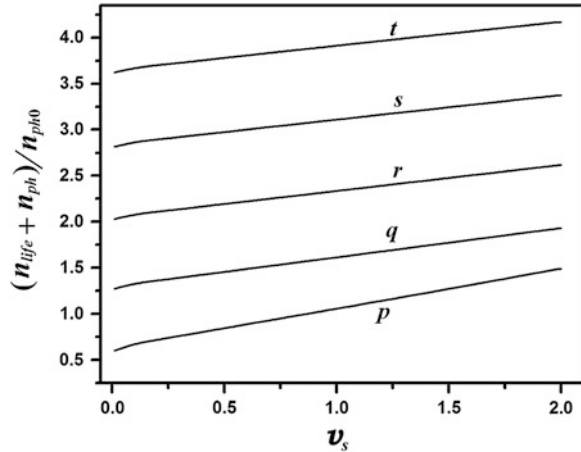


Fig. 2.29 Dependence of $((n_{life} + n_{ph})/n_{ph0})$ with dimensionless surface potential (v_s), for Case-II, $a = 10$ nm, $W_a = 10$ eV, $\mu_d = 5$ with $T = 300$ K. The labels on the curves p , q , r , s and t correspond to $\xi = 0.1$, 0.2 , 0.3 , 0.4 , and 0.5 , respectively (after Mishra et al. [28], courtesy authors and publishers AIP)



results are in conformance with the transmission coefficient curves illustrated in Fig. 2.19. Figure 2.29 displays the fact that light induced field emission (*life*) current significantly contributes to the total emission current ($n_t = n_{ph} + n_{life}$) with increasing v_s ; it is interesting to point out that the total current enhances by a factor of about 2.1 from its initial value (at $v_s = 0$) for the chosen set of parameters.

2.9 Mie's Theory of Light Scattering by Spherical Particles

For large particles, the power incident on a sphere of radius a from a beam of irradiation I is simply

$$P_a = \pi a^2 I.$$

On account of diffraction and scattering, the above equation gets modified to

$$P_a = M_f(a, N, \lambda) \pi a^2 I$$

where the Mie factor M_f depends on a , and the complex refractive index $N = N_1 + iN_2$ of the sphere for the radiation of wavelength λ .

The theory for the interaction of the spherical particles with electromagnetic radiation has been given by *Mie* [27] and elucidated in the excellent books by Stratton [54], Born and Wolf [62], Goody [63] and Van de Hulst [56]. In this section only the results, obtained by Mie [27] have been stated; for a derivation the reader is referred to the cited sources.

The power S of light incident per unit area, normal to the direction of incidence is

$$S = (E_0^2/2)(\epsilon_m/\mu_m)^{1/2}, \quad (2.92)$$

where E_0 is the amplitude of the electric vector, and $\epsilon_m/\epsilon_m\mu_m\cdot\mu_m$ are the dielectric and magnetic permittivity of the medium.

The scattered power W_s is given by

$$W_s = \pi \frac{E_0^2}{k_m^2} (\epsilon_m/\mu_m)^{1/2} \sum_{n=1}^{n=\infty} (2n+1) (|a_n|^2 + |b_n|^2) \quad (2.93)$$

where $k_m = 2\pi/\lambda_m$.

λ_m is the wavelength of the incident radiation in the medium in which the sphere is situated,

$$a_n = - \frac{\mu_s j_n(N\rho) [\rho j_n(\rho)]' - \mu_m j_n(\rho) [N \rho j_n(N\rho)]'}{\mu_s j_n(N\rho) [\rho h_n^{(1)}(\rho)]' - \mu_m h_n^{(1)}(\rho) [N \rho j_n(N\rho)]'}, \quad (2.94a)$$

$$b_n = - \frac{\mu_s j_n(\rho) [N \rho j_n(N\rho)]' - \mu_m N^2 j_n(N\rho) [\rho j_n(N\rho)]'}{\mu_s h_n^{(1)}(\rho) [N \rho j_n(N\rho)]' - \mu_m N^2 j_n(N\rho) [\rho h_n^{(1)}(\rho)]'}, \quad (2.94b)$$

$\rho = k_m a$, N is the complex refractive index of the sphere, relative to the medium

$$j_n(x) = (\pi/2x)^{1/2} J_{n+1/2}(x),$$

$J_m(x)$ is the *Bessel function* of order m ,

$$h_n^{(1)}(x) = (\pi/2x)^{1/2} H_{n+1/2}^{(1)}(x),$$

and $H_{n+1/2}^{(1)}(x)$ is *Henkel function*.

The sum of absorbed and scattered power W_t is given by

$$W_t = \frac{\pi E_0^2}{k_m^2} \left(\frac{\epsilon_m}{\mu_m} \right)^{1/2} \operatorname{Re} \left\{ \sum_{n=1}^{n=\infty} (2n+1)(a_n + b_n) \right\} \quad (2.95)$$

The efficiency factors for scattering Q_s and for scattering cum absorption (total) Q_t are defined as

$$Q_s = (W_s / \pi a^2 S) \quad (2.96a)$$

and

$$Q_t = (W_t / \pi a^2 S) \quad (2.96b)$$

The efficiency factor corresponding to absorption Q_a is given by

$$Q_a = Q_t - Q_s \quad (2.96c)$$

The parameters Q_a , Q_s and Q_t have been tabulated in two books. (*National Bureau of Standards* 1940 and Wickramasinghe [61]).

A user friendly *Mie Calculator*, made available by *Scott Prahl* (on website: http://omlc.orgi.edu/calc/mie_calc.html); may be used for computation of Q_a , Q_s and Q_t . Values corresponding to ice and silicates have been tabulated by Dorschner [6].

Appendix A

Electron Transmission Coefficient Across a Negatively Charged Cylindrical Surface (After Mishra et al. [28], Sodha and Dubey [45])

Sodha and Dixit [42] have evaluated the tunneling probability of an electron in the case of a negatively charged cylindrical surface by following a formalism, proposed by Ghatak et al. [16] and [35]. This approximation is better than *Born's approximation*, but it is not valid when $E_r > 0.7 V_s$. In this section, the case of the cylindrical surface is analyzed on the same lines as in the case of spherical surface.

Assuming that the electron potential energy is zero at $r \geq \lambda_D$, the electron potential energy in and out of the surface is given by

$$v(\rho) = (v_s - 1) \quad \text{for } \rho < 1 \quad (\text{Region-I}) \quad (2.97a)$$

$$v(\rho) = v_s \left(\frac{\ln[\mu_d / \rho]}{\ln[\mu_d]} \right) \exp[-(\rho - 1)/\mu_d] \quad \text{for } 1 < \rho < \rho_n \quad (\text{Region-II}) \quad (2.97b)$$

and

$$v(\rho) = 0 \quad \text{for } \rho > \rho_n \quad (\text{Region-III}) \quad (2.97c)$$

where $v(\rho_n) = 0.05 v_s$ and the symbols are the same as in the case of a spherical surface.

Substituting in

$$\Psi = r^{1/2} \psi(r) \exp(\pm i n \theta) \exp(i c z),$$

time independent *Schrödinger's* equation, interpreting n and c in term of the θ and z component of the linear momentum of an electron, one obtains [45]

$$\frac{d^2 \psi}{dr^2} + \frac{8\pi^2 m_e}{h^2} (E_r - V(r)) \psi = 0$$

or

$$\frac{d^2 \psi}{d\rho^2} + \beta(\varepsilon_r - v(\rho)) \psi = 0$$

where the nomenclature is the same as in the spherical case.

Substituting for $v(\rho)$ from (2.97) in the above equation one obtains

$$\frac{d^2 \psi}{d\rho^2} + \beta(\varepsilon_r - v_s + 1) \psi = 0 \quad \text{for } \rho < 1 \quad (\text{Region-I}), \quad (2.98a)$$

$$\frac{d^2 \psi}{d\rho^2} + \beta \left\{ \varepsilon_r - v_s \left(\frac{\ln[\mu_d/\rho]}{\ln[\mu_d]} \right) \exp[-(\rho - 1)/\mu_d] \right\} \psi = 0 \quad \text{for } 1 < \rho < \rho_n \quad (2.98b)$$

(Region-II)

and

$$\frac{d^2 \psi}{d\rho^2} + \beta \varepsilon_r \psi = 0 \quad \text{for } \rho > \rho_n \quad (\text{Region-III}). \quad (2.98c)$$

It may be noticed that the dependences of $v(\rho)$ on ρ , are very close (for $\mu_d > 5$) for the spherical and cylindrical surfaces, corresponding to the regions when $1 < \rho < 3$ and $v_s < v(\rho) < 0.2 v_s$. Since these are the main regions, contributing to the transmission probability the ε_r dependence of $D_e(\varepsilon_r)$ and $D_a(\varepsilon_r)$ should also be almost the same in the two cases. Hence, the electron current for given v_s , μ_d and a will also be the same in both cases. Computations for the two cases support this conclusion.

Appendix B

Secondary Emission from Cylindrical Particles

Chow et al. [4] have analyzed secondary electron emission from a cylindrical grain on account of the incidence of a high energy beam of (primary) electrons, propagating in a direction parallel to the axis of the grain. This restriction puts a severe limitation on the application of this model to complex plasma kinetics.

The phenomenon of secondary electron emission from the surface of an infinitely long cylindrical grain for oblique incidence of primary electrons has been analyzed herein. Specifically, the ratio δ_0 of the number of emitted secondary electrons to that of accreting incident primary (high energy) electrons has been evaluated for an electrically neutral particle. The multiplying factor for a charged particle has been given. For typical parameters, numerical results have been obtained and discussed.

Consider the incidence of a uniform electron beam on an infinitely long cylinder, with its axis at an angle λ with the direction of propagation of the beam. Fig. A.1 represents the cross section of the cylinder at an angle λ to the axis, which is an ellipse with semi major axis $a \sec \lambda$ and semi minor axis a , where a is the radius of the cylinder; the primary electrons travel along chords, parallel to the major axis. Thus, the typical path of a primary electron is AB , parallel to the major axis at a distance ρ from the center O .

Using simple coordinate geometry

$$AB = 2(a^2 - \rho^2)^{1/2} \sec \lambda = 2x_1. \quad (A1)$$

The distance r_1 of point P from the axis of the cylinder is given by

$$r_1^2 = (x_1 - x)^2 \sin^2 \lambda + \rho^2 \quad (A2)$$

where $(x_1 - x) \sin \lambda$ is the projection of $(x_1 - x)$ on a plane, normal to the axis.

If one chooses a system of coordinates with P (at a distance r_1 from the axis) as origin, $\Phi = 0$ as the perpendicular from P on the axis and $\theta = 0$ in the plane having P and normal to the axis, the distance l of any point on the cylinder to P can be shown to be given by

$$l = (r_1^2 + a^2 + 2r_1 a \cos \varphi)^{1/2} \sec \theta \quad (A3)$$

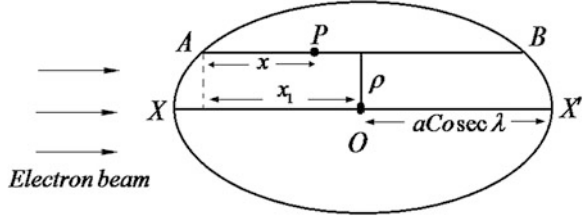
Equations (2.56) and (2.57) are valid in this case also, where l is given by (A3).

The number of secondary electrons generated by a primary electron in motion along AB is

$$F(\rho) = (1 - \eta_{se}) \int_0^X dn_s = (1 - \eta_{se}) \frac{K \alpha^{1/2}}{2} \int_0^X (x_m - x)^{-1/2} f(x, \rho) dx, \quad (A4)$$

where

Fig. A.1 Oblique incidence of electrons on a cylindrical particle



$$X = 2x_1 \quad \text{if } x_m > 2x_1 \text{ or } \rho > \rho_m, \quad (\text{A5a})$$

$$X = x_m \quad \text{if } x_m < 2x_1 \text{ or } \rho < \rho_m, \quad (\text{B5b})$$

$2x_1$ is given by (A1).

η_{se} is sticking coefficient of electrons on the particle surface and

$$\rho_m^2 = a^2 - (x_m \sin \lambda / 2)^2 \quad (\text{A5c})$$

If $x_m < 2a \cos \sec \lambda$, ρ_m is real and positive and the limits of x are obtained from (A5a) and (B5b) and if $x_m > 2a \cos \sec \lambda$, the limits are given by (A5a).

Hence, the mean number of secondary electrons $\delta_0(\lambda)$ generated by the motion of a primary electron in the cylindrical particle

$$\delta_0(\lambda) = (1/2a) \int_{-a}^a F(\rho) d\rho = (1/a) \int_0^a F(\rho) d\rho \quad (\text{A6})$$

where $F(\rho)$ is given by (A4).

The corresponding mean number of electrons stuck ($x_m < 2x_1$) per primary electron is given by

$$\delta_{st}(\lambda) = (1 - \eta_{se})(2\rho_m/2a) = (1 - \eta_{se})(\rho_m/a) \quad (\text{A7})$$

In case the particle is at an electric potential V_s with respect to the surroundings one has (Sodha et al. 2005)

$$\delta(v_s, \lambda) = \delta_0(\lambda) \quad \text{for } v_s \geq 0 \quad (\text{A8a})$$

and

$$\delta(v_s, \lambda) = \exp(-v_s) \{ (2/\pi^{1/2}) v_s^{1/2} + \exp(v_s) \operatorname{erfc}(v_s^{1/2}) \} \delta_0(\lambda) \quad \text{for } v_s < 0 \quad (\text{A8b})$$

where $v_s = eV_s/kT_s$, e is the electronic charge, k is Boltzmann's constant and T_s is the temperature of the particle.

In general, the angle λ , between the incoming electron direction and the axis of the cylinder varies at random. Hence

$$\overline{\delta_0} = \int_0^{\pi/2} \delta_0(\sin \lambda / 2) d\lambda \quad (\text{A9a})$$

and

$$\overline{\delta_{st}} = \int_0^{\pi/2} \delta_{st}(\sin\lambda/2) d\lambda = ((1 - \eta_{se})/a) \int_0^{\pi/2} \rho_m(\sin\lambda/2) d\lambda, \quad (\text{A9b})$$

where $(\sin\lambda/2)d\lambda$ is the solid angle contained between cones making angle between λ and $(\lambda + d\lambda)$ with the axis divided by 4π .

From (8Aa) and (8Ab), one can write

$$\overline{\delta}(v_s) = \overline{\delta}_0 \quad \text{for } v_s \geq 0 \quad (\text{A8c})$$

and

$$\overline{\delta}(v_s, \lambda) = \exp(-v_s) \{ (2/\pi^{1/2}) v_s^{1/2} + \exp(v_s) \text{erfc}(v_s^{1/2}) \} \overline{\delta}_0(\lambda) \quad \text{for } v_s < 0. \quad (\text{A8d})$$

The energy (kT_e) distribution of the electrons incident on the particle per unit time is given by

$$n_e(v_p) dv_p = \pi a l (2kT_e/m\pi)^{1/2} n_e(v_p - v_s) \exp(-v_p) dv_p, \quad (\text{2.10})$$

where $v_p = (V_P/kT_e)$.

Hence, the number of secondary electrons emitted by the particle per unit time is

$$n_{\text{see}} = \int_0^\infty n_e(v_p) \overline{\delta}(v_s, v_p) dv_p \quad \text{for } v_s < 0 \quad (\text{2.11a})$$

and

$$n_{\text{see}} = \int_{v_s}^\infty n_e(v_p) \overline{\delta}(v_s, v_p) dv_p \quad \text{for } v_s \geq 0. \quad (\text{2.11b})$$

The number of electrons stuck in the particles per unit time is

$$n_{\text{stuck}} = \int_0^{v'} n_e(v_p) \overline{\delta}_{st}(v_p) dv_p \quad \text{for } v_s < 0 \quad (\text{2.12a})$$

$$n_{\text{stuck}} = \int_{v_s}^{v'} n_e(v_p) \overline{\delta}_{st}(v_p) dv_p \quad \text{for } v_s \geq 0 \quad (\text{2.12b})$$

where

$$v' = V'/kT_e = v_s(T_s/T_e) + \left[(2a\alpha \sec \lambda)^{1/2} / kT_e \right], \quad (\text{2.12c})$$

corresponding to the primary electron energy needed to traverse a distance $2a \sec \lambda$; in other words,

$$x_m(V') = 2a \sec \lambda.$$

References

1. S. Agarwal, S. Misra, S.K. Mishra, M.S. Sodha, Can. J. Phys. **90**, 265 (2012)
2. C.N. Berglund, W.E. Spicer, Phys. Rev. **4A**, A1030 (1964)
3. H. Bruining, Thesis, Leydew, *Die Sekandar-Electron Emission Festa Korper*, (Springer Berlin, 1942). p. 60
4. V.W. Chow, M. Rosenberg, Planet. Space Sci. **43**, 613 (1995)
5. V.W. Chow, D.A. Mendis, M. Rosenberg, J. Geophys. Res. **98**, 19065 (1993)
6. J. Dorschner, Astron. Nachr. Bd. **292**, H. 2 (1970)
7. B.T. Draine, Astrophys. J. Suppl. Ser. **36**, 595 (1978)
8. B.T. Draine, B. Sutin, Astrophys. J. **320**, 803 (1987)
9. J.W. Dewdney, Phys. Rev. **125**, 399 (1962)
10. P.K. Dubey, J. Phys. D **3**, 145 (1970)
11. L.A. Dubridge, Phys. Rev. **43**, 727 (1933)
12. R.G. Forbes, J.H.B. Deane, Proc. Roy. Soc. Lond. **A467**, 2927 (2011)
13. R.H. Fowler, Phys. Rev. **38**, 45 (1931)
14. R.H. Fowler, *Statistical Mechanics: The Theory of the Properties of Matter in Equilibrium* (Cambridge University Press, London, 1955)
15. R.H. Fowler, L.W. Nordheim, Proc. Roy. Soc. Lond. **A112**, 781 (1928)
16. A. Ghatak, R.L. Gallawa, I.C. Goyal, IEEE J. Quat. Electr. **28**, 400 (1992)
17. A. Ghatak, S. Lokanathan, *Quantum Mechanics, Theory and Applications* (Macmillan, New Delhi, 2005)
18. O. Hachenberg, W. Brauer, Adv. Electron Phys. **11**, 413 (1959)
19. C. Herring, M.H. Nichols, Rev. Mod. Phys. **21**, 185 (1949)
20. J.H. Jonker, Phillips Res. Repts. **7**, 1 (1952)
21. K. Iwami, A. Iuzuka, N. Umeda, J. Vac. Sci. Technol. B, **29**, 028103 (2011)
22. R.O. Jenkins, W.G. Trodden, *Electron and Ion Emission from Solids* (Dover Publications, New York, 1965)
23. S. Kher, A. Dixit, D. N. Rawat, M.S. Sodha Appl. Phys. Lett. **96**, 044101 (2010)
24. B.A. Klumov, S.I. Popel, R. Bingham, JETP Lett. **72**, 364 (2000)
25. D.R. Lide, Editor-in-chief, *CRC Handbook of Chemistry and Physics*, 89th edn. (CRC Press, New York, 2008–2009)
26. N. Meyer Vernet, Astron. Astrophys. **105**, 98 (1982)
27. G. Mie, Ann. Physik [4], **25**, 377 (1908)
28. S.K. Mishra, S. Misra, M.S. Sodha, Phys. Plasmas **19**, 073705 (2012)
29. S.K. Mishra, M.S. Sodha, S. Srivastava, Astrophys. Space Sci. **344**, 193 (2013)
30. S. Misra, M.S. Sodha, Can. Phys. Under publication
31. S. Misra, S.K. Mishra, M.S. Sodha Phys. Plasma **20**, 013702 (2013)
32. L.W. Nordheim, Proc. Roy. Soc. Lond. **A121**, 788 (1928)
33. L. Page, N.I. Adams, *Principles of Electricity* (D Van Nostranel, New York, 1931). p. 103
34. G. Prakash, Can. J. Phys. **8**, 617 (2010)
35. S. Roy, A.K. Ghatak, I.C. Goyal, IEEE J. Quant. Electr. **29**, 340 (1993)
36. W. Schottky, Z. Phys. **14**, 63 (1923)
37. F. Seitz, *Modern Theory of Solids* (Mc Graw Hill Book Co., New York, 1940)
38. M.S. Sodha, J. Appl. Phys. **32**, 2059 (1961)
39. M.S. Sodha, Brit. J. Appl. Phys. **14**, 172 (1963)
40. M.S. Sodha, A. Dixit, J. Appl. Phys. **104**, 064909 (2008)
41. M.S. Sodha, A. Dixit, S. Srivastava, Appl. Phys. Lett. **94**, 251501 (2009a)
42. M.S. Sodha, A. Dixit, J. Appl. Phys. **105**, 034909 (2009b)
43. M.S. Sodha, A. Dixit, S.K. Agarwal, Can. J. Phys. **87**, 175 (2009c)
44. M. S. Sodha, A. Dixit, S. Srivastava, Phys. Rev. E **79**, 046407 (2009d); erratum E **80**, 06990 (2010)
45. M.S. Sodha, P.K. Dubey, Brit. J. Appl. Phys. D **2**, 1617 (1969)

46. M.S. Sodha, S. Guha, *Physics of Colloidal Plasmas*, vol. 4 eds. by A. Simon, W.B. Thompson. *In Advances Plasma Physics* (InterScience New York, 1971). pp. 219–369
47. M.S. Sodha, P.K. Kaw, Brit. J. Appl. Phys. D **1**, 1303 (1968)
48. M.S. Sodha, S.K. Mishra, Phys. Plasmas **18**, 083708 (2011)
49. M.S. Sodha, S.K. Mishra, S. Misra, Phys. Plasmas **16**, 123701 (2009e)
50. M.S. Sodha, S. Sharma, Brit. J. Appl. Phys. D **18**, 1127 (1967)
51. M.S. Sodha, S. Srivastava, Phys. Lett. A **374**, 4733 (2010)
52. W.E. Spicer, Phys. Rev. **112**, 114 (1958)
53. W.E. Spicer, A Herrera-Gomez, Modern Theory and Applications of Photocathodes. *Paper Presented at SPIE's International Symposium on Optics, Imaging and Instrumentation*, San Diego, CA, July 11–16, 1993; SLAC-PUB-6306; SLAC/SSRL-0042, August 1993 (A-SSRL-H)
54. J.A. Stratton, *Electromagnetic Theory* (Mc Graw Hill, New York, 1941), pp. 563–573
55. E.J. Sternglass, *Scientific Paper 1773* (Westinghouse Research lab, Pittsburgh, 1954)
56. H.C. Van de Hulst, *Light Scattering by Small Particles* (Wiley, New York, 1957)
57. W.D. Watson, Astrophys. J. **176**, 103 (1972)
58. W.D. Watson, J. Opt. Soc. Am. **63**, 164 (1973)
59. R. Whiddington, Proc. Roy. Soc. **A86**, 360 (1912)
60. E.C. Whipple, Rep. Prog. Phys. **44**, 1197 (1981)
61. N.C. Wikramsinghe, *Light Scattering Functions for Small Particles* (Wiley, New York, 1973)
62. M. Born, E. Wolf, *Principles of Optics*, Chapter XIII, McMillan, New York (1964)
63. R.M. Goody, *Atmospheric Radiation I. Theoretical Basis*, Chapter 7, Oxford University Press (Clarendon, London and New York, 1964)
64. L. Spitzer, Astrophys. J. **93**, 369 (1948)
65. B.T. Draine, E.E. Salpeter, Astrophys. J. **231**, 77 (1979)
66. J.L. Puget, A. Leger, Ann. Rev. Astron. Astrophys. **27**, 161 (1989)
67. R.Z. Sagdeev, E.N. Evlanov, M.N. Formenkova, O.F. Prilutskii, B.V. Zubov, Adv. Space Res. **9**, 263 (1989)
68. M.M. Abbas, D. Tankosio, P.D. Craven, A.C. McClair, J.F. Spann, Astrophys. J. **T18**, 795 (2010)



<http://www.springer.com/978-81-322-1819-7>

Kinetics of Complex Plasmas

Sodha, M.S.

2014, XIX, 298 p. 101 illus., Hardcover

ISBN: 978-81-322-1819-7